Camper, S.A., 2000. The motor and tail regions of myosin XV are critical for normal structure and function of auditory and vestibular hair cells. Hum. Mol. Genet. 9, 1729–1738.

Anniko, M., Sobin, A., Wersall, J., 1980. Vestibular hair cell pathology in the Shaker-2 mouse. Arch. Otorhinolaryngol. 226, 45–50.

Belyantseva, I.A., Boger, E.T., Friedman, T.B., 2003. Myosin XVa localizes to the tips of inner ear sensory cell stereocilia and is essential for staircase formation of the hair bundle. Proc. Natl. Acad. Sci. USA 100, 13958–13963.

Belyantseva, I.A., Boger, E.T., Naz, S., Frolenkov, G.I., Sellers, J.R., Ahmed, Z.M., Griffith, A.J., Friedman, T.B., 2005. Myosin-XVa is required for tip localization of whirlin and differential elongation of hair-cell stereocilia. Nat. Cell. Biol. 7, 148–156.

Beyer, L.A., Odeh, H., Probst, F.J., Lambert, E.H., Dolan, D.F., Camper, S.A., Kohrman, D.C., Raphael, Y., 2000. Hair cells in the inner ear of the pirouette and shaker 2 mutant mice. J. Neurocytol. 29, 227–240.

Delprat, B., Michel, V., Goodyear, R., Yamasaki, Y., Michalski, N., El-Amraoui, A., Perfettini, I., Legrain, P., Richardson, G., Hardelin, J.P., Petit, C., 2005. Myosin XVa and whirlin, two deafness gene products required for hair bundle growth, are located at the stereocilia tips and interact directly. Hum. Mol. Genet. 14, 401–410.

Deol, M.S., 1952. The anomalies of the labyrinth of the mutants varitint-waddler, shaker-2 and jerker in the mouse. J. Genet. 52, 562–588.

Dobrovolskaia-Zavasdkaia, N., 1928. L'irradiation des testicules et l'heredite chez la souris. Arch. Biol. (Liege) 38, 457–501.

FitzPatrick, D.R., 2005. Transcriptional consequences of autosomal trisomy: primary gene dosage with complex downstream effects. Trends Genet. 21, 249–253.

Friedman, T.B., Griffith, A.J., 2003. Human nonsyndromic sensorineural deafness. Annu. Rev. Genom. Hum. Genet. 4, 341–402.

Friedman, T.B., Hinnant, J.T., Ghosh, M., Boger, E.T., Riazuddin, S., Lupski, J.R., Potocki, L., Wilcox, E.R., 2002. DFNB3, spectrum of MYO15A recessive mutant alleles and an emerging genotype-phenotype correlation. Adv. Otorhinolaryngol. 61, 124–130.

Haider, N.B., Ikeda, A., Naggert, J.K., Nishina, P.M., 2002. Genetic modifiers of vision and hearing. Hum. Mol. Genet. 11, 1195–1206.

Kanzaki, S., Beyer, L.A., Canlon, B., Meixner, W.M., Raphael, Y., 2002. The cytocaud: a hair cell pathology in the waltzing Guinea pig. Audiol. Neurootol. 7, 289–297.

Karolyi, I.J., Probst, F.J., Beyer, L., Odeh, H., Dootz, G., Cha, K.B., Martin, D.M., Avraham, K.B., Kohrman, D., Dolan, D.F., Raphael, Y., Camper, S.A., 2003. Myo15 function is distinct from Myo6, Myo7a, and pirouette genes in development of cochlear stereocilia. Hum. Mol. Genet..

Keithley, E.M., Feldman, M.L., 1982. Hair cell counts in an age-graded series of rat cochleas. Hear. Res. 8, 249–262.

Liang, Y., Wang, A., Probst, F.J., Arhya, I.N., Barber, T.D., Chen, K.S., Deshmukh, D., Dolan, D.F., Hinnant, J.T., Carter, L.E., Jain, P.K., Lalwani, A.K., Li, X.C., Lupski, J.R., Moeljopawiro, S., Morell, R., Negrini, C., Wilcox, E.R., Winata, S., Camper, S.A., Friedman, T.B., 1998. Genetic mapping refines DFNB3 to 17p11.2, suggests multiple alleles of DFNB3, and supports homology to the mouse model shaker-2. Am. J. Hum. Genet. 62, 904–915.

Liang, Y., Wang, A., Belyantseva, I.A., Anderson, D.W., Probst, F.J., Barber, T.D., Miller, W., Touchman, J.W., Jin, L., Sullivan, S.L., Sellers, J.R., Camper, S.A., Lloyd, R.V., Kachar, B., Friedman, T.B., Fridell, R.A., 1999. Characterization of the human and mouse unconventional myosin XV genes responsible for hereditary deafness DFNB3 and shaker 2. Genomics 61, 243–258.

Liburd, N., Ghosh, M., Riazuddin, S., Naz, S., Khan, S., Ahmed, Z., Liang, Y., Menon, P.S., Smith, T., Smith, A.C., Chen, K.S., Lupski, J.R., Wilcox, E.R., Potocki, L., Friedman, T.B., 2001. Novel mutations of MYO15A associated with profound deafness in consanguineous families and moderately severe hearing loss in a patient with Smith-Magenis syndrome. Hum. Genet. 109, 535–541.

Maeda, Y., Fukushima, K., Nishizaki, K., Smith, R.J., 2005. In vitro and in vivo suppression of GJB2 expression by RNA interference. Hum. Mol. Genet..

Mburu, P., Mustapha, M., Varela, A., Weil, D., El-Amraoui, A., Holme, R.H., Rump, A., Hardisty, R.E., Blanchard, S., Coimbra, R.S., Perfettini, I., Parkinson, N., Mallon, A.M., Glenister, P., Rogers, M.J., Paige, A.J., Moir, L., Clay, J., Rosenthal, A., Liu, X.Z., Blanco, G., Steel, K.P., Petit, C., Brown, S.D., 2003. Defects in whirlin, a PDZ domain molecule involved in stereocilia elongation, cause deafness in the whirler mouse and families with DFNB31. Nat. Genet. 34, 421–428.

Morton, C.C., 2002. Genetics, genomics and gene discovery in the auditory system. Hum. Mol. Genet. 11, 1229–1240.

Niedzielski, A.S., Schacht, J., 1991. Phospholipid metabolism in the cochlea: differences between base and apex. Hear. Res. 57, 107–112.

Ohlemiller, K.K., Wright, J.S., Heidbreder, A.F., 2000. Vulnerability to noise-induced hearing loss in 'middle-aged' and young adult mice: a dose–response approach in CBA, C57BL, and BALB inbred strains. Hear. Res. 149, 239–247.

Osborne, M.P., Comis, S.D., Pickles, J.O., 1984. Morphology and cross-linkage of stereocilia in the guinea-pig labyrinth examined without the use of osmium as a fixative. Cell Tissue Res. 237, 43–48.

Probst, F.J., Fridell, R.A., Raphael, Y., Saunders, T.L., Wang, A., Liang, Y., Morell, R.J., Touchman, J.W., Lyons, R.H., Noben-Trauth, K., Friedman, T.B., Camper, S.A., 1998. Correction of deafness in shaker-2 mice by an unconventional myosin in a BAC transgene. Science 280, 1444–1447.

Raphael, Y., Athey, B.D., Wang, Y., Lee, M.K., Altschuler, R.A., 1994. F-actin, tubulin and spectrin in the organ of Corti: comparative distribution in different cell types and mammalian species. Hear. Res. 76, 173–187.

Raphael, Y., Kobayashi, K.N., Dootz, G.A., Beyer, L.A., Dolan, D.F., Burmeister, M., 2001. Severe vestibular and auditory impairment in three alleles of Ames waltzer (av) mice. Hear. Res. 151, 237–249.

Schedl, A., Ross, A., Lee, M., Engelkamp, D., Rashbass, P., van Heyningen, V., Hastie, N.D., 1996. Influence of PAX6 gene dosage on development: overexpression causes severe eye abnormalities. Cell 86, 71–82.

Schneider, M.E., Belyantseva, I.A., Azevedo, R.B., Kachar, B., 2002. Rapid renewal of auditory hair bundles. Nature 418, 837–838.

Snell, G.D., Law, L.W., 1939. A linkage between *shaker-2* and *wavy-2* in the house mouse. J. Hered. 30, 447.

Sobin, A., Anniko, M., Flock, A., 1982. Rods of actin filaments in type I hair cells of the Shaker-2 mouse. Arch. Otorhinolaryngol. 236, 1–6.

Wang, A., Liang, Y., Fridell, R.A., Probst, F.J., Wilcox, E.R., Touchman, J.W., Morton, C.C., Morell, R.J., Noben-Trauth, K., Camper, S.A., Friedman, T.B., 1998. Association of unconventional myosin MYO15 mutations with human nonsyndromic deafness DFNB3. Science 280, 1447–1451.

Yu, R.N., Ito, M., Saunders, T.L., Camper, S.A., Jameson, J.L., 1998. Role of Ahch in gonadal development and gametogenesis. Nat. Genet. 20, 353–357.

ELSEVIER

Bone xx (2006) xxx–xxx

BONE

www.elsevier.com/locate/bone

Rapid Communication

Resorption of auditory ossicles and hearing loss in mice lacking osteoprotegerin

Sho Kanzaki [a], Masako Ito [c], Yasunari Takada [b], Kaoru Ogawa [a], Koichi Matsuo [b,*]

[a] *Department of Otolaryngology, School of Medicine, Keio University, 35 Shinanomachi, Shinjuku-ku, Tokyo 160-8582, Japan*
[b] *Department of Microbiology and Immunology, School of Medicine, Keio University, 35 Shinanomachi, Shinjuku-ku, Tokyo 160-8582, Japan*
[c] *Department of Radiology, Nagasaki University School of Medicine, 1-7-1 Sakamoto, 852-8501 Nagasaki, Japan*

Received 15 September 2005; revised 16 January 2006; accepted 31 January 2006

Abstract

Bones conduct sound in the middle ear. The three ossicles—the malleus, incus, and stapes—form a chain that transmits vibrations from the tympanic membrane to the oval window of the inner ear. Little is known about bone remodeling events in these ossicles and about potential effects of osteoporosis on hearing loss. Osteoclastic bone resorption is enhanced in $Opg^{-/-}$ mice lacking osteoprotegerin, which is a soluble decoy receptor for the osteoclastogenic cytokine RANKL. We asked whether auditory ossicles are resorbed in $Opg^{-/-}$ mice, and whether these mice suffer from impaired auditory function. All three ossicles in $Opg^{-/-}$ mice showed thinning, especially at the malleal manubrium and incus body. Most notably, unlike in the case in wild-type mice, the junction between the stapes and the otic capsule was fixed in $Opg^{-/-}$ mice, and the stapedial footplate was thinner and broader. Radiological analyses revealed that malleal cortical thickness was positively correlated with tibial bone mineral density in $Opg^{-/-}$ and control littermate mice. Furthermore, progressive hearing loss was detected in $Opg^{-/-}$ mice starting at 6 to 15 weeks of age. These data suggest that osteoprotegerin plays a crucial role in hearing by protecting the auditory ossicles and otic capsule from osteoclastic bone resorption.

Keywords: Bone remodeling; Osteoclast; Osteoprotegerin; Hearing loss; Auditory ossicles

Introduction

The three ossicles in the middle ear, the malleus, incus, and stapes, are formed mainly by endochondral ossification of the mesenchyme from the first and second branchial arches [1,2]. The manubrium (handle) of the malleus attaches to the tympanic membrane, while the footplate of the stapes attaches to the oval window of the cochlea. The stapedial foot is mobile and transmits vibrations to the perilymph, the fluid in the inner ear. The inner ear is contained in the otic capsule of the temporal bone, which is the hardest bone in the body.

Bone mineral density (BMD) is determined by the balance between bone resorption by osteoclasts and formation by osteoblasts. Genetic studies of osteopetrotic mice reveal a number of molecules essential for osteoclastogenesis. Osteoclasts differentiate from precursors of the monocyte–macrophage lineage in the presence of the two membrane bound cytokines, macrophage-colony stimulating factor (M-CSF) and RANKL (receptor activator of nuclear factor-κB ligand, also called osteoclast differentiation factor or TRANCE) [3]. The RANKL receptor is a tumor necrosis factor receptor superfamily member known as RANK encoded by the *Tnfrsf11A* gene. RANK signaling in osteoclast precursors activates a series of osteoclastogenic transcription factors including NF-κB, c-Fos/AP-1, and NFATc1 [4–9]. The osteoclastogenic activity of RANKL is masked by the soluble decoy receptor osteoprotegerin (OPG, also called osteoclast inhibitory factor), encoded by *Tnfrsf11B* [10,11]. In bone remodeling, BMD is maintained by a coupling of osteoclastic bone resorption with subsequent osteoblastic formation [12].

In human populations, the incidence of osteoporotic hip fracture increases exponentially with age [13]. Age-related hearing loss, or presbycusis, affects more than one third of individuals above the age of 75 [14]. Although a link between

* Corresponding author. Fax: +81 3 5360 1508.
E-mail address: matsuo@sc.itc.keio.ac.jp (K. Matsuo).

8756-3282/$ - see front matter © 2006 Elsevier Inc. All rights reserved.
doi:10.1016/j.bone.2006.01.155

osteoporosis and hearing loss has been suggested [15–17], recent epidemiological studies reveal no correlation of hearing loss and osteoporosis in elderly women [18], a finding that seems counterintuitive given that hearing largely depends on bone.

$Opg^{-/-}$ mice develop osteopenia due to enhanced differentiation of osteoclasts [19–22]. To gain deeper insight into the role of bone remodeling in hearing, we asked if auditory ossicles are susceptible to osteoclastic bone resorption in $Opg^{-/-}$ mice and whether auditory function is impaired.

Materials and methods

Mice

Female *Opg* $^{-/-}$ and heterozygous control mice on a C57BL6 background were purchased from Clea Japan. All experiments were conducted in accordance with institutional review board-approved protocols.

Morphological analyses

Mouse skulls were fixed in 4% paraformaldehyde. For macroscopic analysis, auditory ossicles were isolated by removing the temporal bone, stained for tartrate-resistant acid phosphatase (TRAP) activity using the Leukocyte Acid Phosphatase Kit (Sigma), and observed using a SMZ1500, stereoscopic zoom microscope configured with the Eclipse 90i digital camera system (Nikon). For histological analysis, skulls were decalcified in 0.5 M EDTA for 1 week, and the temporal bones containing auditory ossicles were trimmed and embedded in paraffin. Frontal sections of 5 μm thickness were stained with hematoxylin–eosin (HE) and for TRAP activity.

Radiographical analyses

Each isolated malleus was embedded in melted 8% gelatin in a segment of a plastic drinking straw. After solidifying the gelatin at 4°C, mallei were scanned using micro-computed tomography (μCT) instrumentation (μCT-40, Scanco Medical AG, Switzerland). Based on two-dimensional data from scanned slices, cortical thickness was calculated by setting the volume of interest (VOI) to the entire malleus. Tibial cortical BMD was measured using a CT scanner (*LaTheta* LCT-100, Aloka, Japan) with isolated bilateral tibiae.

Auditory brain-stem response (ABR) measurement

A needle electrode was subdermally inserted at the vertex along the dorsal midline of the scalp between the external auditory canals. The reference electrode was placed below the pinna of the left ear, and the ground electrode was inserted below the contralateral ear. The sound stimulus consisted of a 1 ms tone burst with a rise–fall time of 0.1 ms. For each stimulus, ABR waveforms were recorded for 12.8 ms at a sampling rate of 40,000 Hz using 50–5000 Hz bandpass filter settings, and waveforms from 256 stimuli at a frequency of 9 Hz were averaged. ABR waveforms were recorded in 5-dB sound pressure level (SPL) intervals down from a maximum amplitude until no waveform could be observed using Scope software of the PowerLab system (PowerLab2/20, AD Instruments, Australia). ABRs were performed on mice aged 6, 10, and 15 weeks at the following frequencies: 2, 4, 12, and 20 kHz. ABRs were measured under anesthesia induced by intraperitoneal injection of 0.01 ml/g body weight of 2.5% avertin. The researcher who measured ABRs was unaware of the identities of the animals.

Statistical analysis

Statistical comparisons were performed using Student's *t* test and analysis of variance, where appropriate.

Results

To examine the morphology of the auditory ossicles in $Opg^{-/-}$ mice, we isolated mallei, incudes, and stapes from the middle ear cavities of 10-week-old $Opg^{-/-}$ mice and from wild-type and heterozygous controls. We observed that the junction between the stapes and the oval window of the cochlea was tighter in $Opg^{-/-}$ mice compared to control mice. Ossicles from $Opg^{-/-}$ and control mice were stained for TRAP activity, which is a marker for osteoclasts and resorption lacunae. Compared to wild-type and heterozygous controls, all three ossicles in $Opg^{-/-}$ mice were more heavily stained for TRAP activity and exhibited thinning, particularly at the malleal manubrium, malleal processus brevis, incus body, and stapedial arch (Fig. 1a). Furthermore, the stapedial footplate was thinner and broader at the periphery in $Opg^{-/-}$ mice (Fig. 1a, Stapes, top view). Such thinner parts of ossicles, especially of the stapes, exhibited intense TRAP staining (Fig. 1a).

To further analyze osteoclasts in the auditory ossicles, histological sections of the temporal bone from wild-type, heterozygous, and $Opg^{-/-}$ mice were stained for TRAP activity. Compared to wild-type and heterozygous controls, TRAP-staining was much stronger in both auditory ossicles and the otic capsule in $Opg^{-/-}$ mice (Fig. 1b and data not shown). We next quantitated the number of TRAP-positive multinucleated cells (MNCs) in wild-type, heterozygous, and $Opg^{-/-}$ mice (Fig. 1c). The number of TRAP-positive MNCs was significantly higher in $Opg^{-/-}$ mice than in controls, suggesting that osteoclastic bone resorption of auditory ossicles is dramatically enhanced in $Opg^{-/-}$ mice.

We also histologically examined the junction between the stapes and the otic capsule in heterozygous and $Opg^{-/-}$ mice. The ligament between the stapedial footplate and otic capsule was intact in heterozygous mice (Fig. 2a), while no ligament was seen in $Opg^{-/-}$ mice, and the junction was replaced with bone tissue fusing the stapes and otic capsule (Fig. 2b).

We next examined the auditory ossicles radiographically. Imaging using μCT of isolated mallei confirmed massive erosion in ossicles of $Opg^{-/-}$ mice, which was not observed in heterozygous mice (Fig. 3a). Based on the μCT images, cortical thickness of mallei was calculated in $Opg^{-/-}$ mice and controls. Malleal cortical thickness observed in $Opg^{-/-}$ mice was significantly lower than that seen in heterozygous controls (Fig. 3b). As expected, tibial cortical BMD of $Opg^{-/-}$ mice was also lower than that seen in heterozygous mice (Fig. 3c). Consistent with the histological data, these

Fig. 1. Excess bone remodeling of auditory ossicles. (a) Biomicroscopic photographs showing auditory ossicles from 10-week-old wild-type (+/+), heterozygous (+/−), and *Opg* $^{-/-}$ (−/−) mice ($n = 6$ or more for each genotype). Ossicles were stained for TRAP activity (red). Arrowheads indicate the malleal manubrium, incus body, and stapedial footplate. Scale bar, 100 μm. (b) Histological sections of auditory ossicles in the middle ear cavity from 15-week-old *Opg* $^{-/-}$ mice ($n = 2$ per genotype). HE and TRAP activity staining is shown. TRAP-positive areas in the malleus (M), incus (I), and stapes (S) are indicated by arrowheads, and those in the otic capsule by arrows. tm, tympanic membrane. Scale bar, 100 μm. (c) The number of TRAP-positive MNCs in mallei from wild-type, heterozygous, and *Opg* $^{-/-}$ mice ($n = 5$ for +/+, $n = 4$ for +/− and −/−). $^{\#}P < 0.001$.

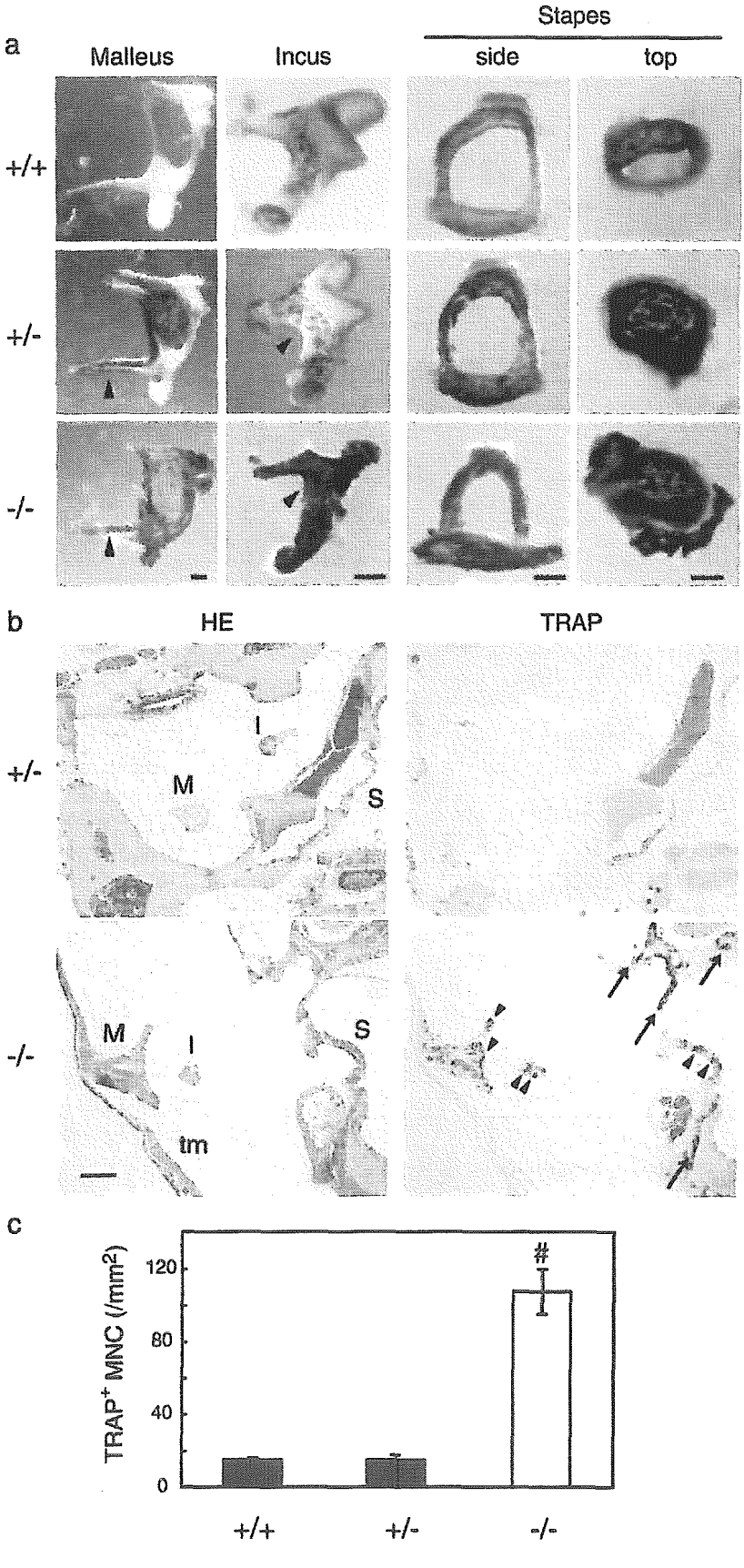
a
Malleus
Incus
Stapes
side
top
+/+
+/-
-/-
b
HE
TRAP
+/-
-/-
M
I
S
tm
c
TRAP+ MNC (/mm2)
120
80
40
0
#
+/+
+/-
-/-

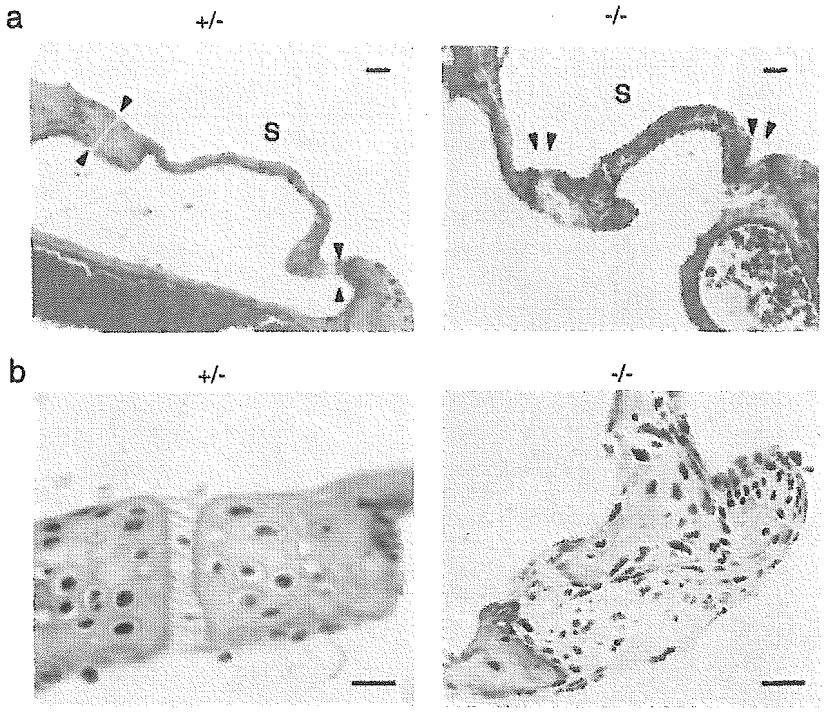

Fig. 2. Histological sections of the stapedial–cochlear junction (arrowheads). Staining is HE (n = 3 for each genotype). Scale bar, 25 μm.

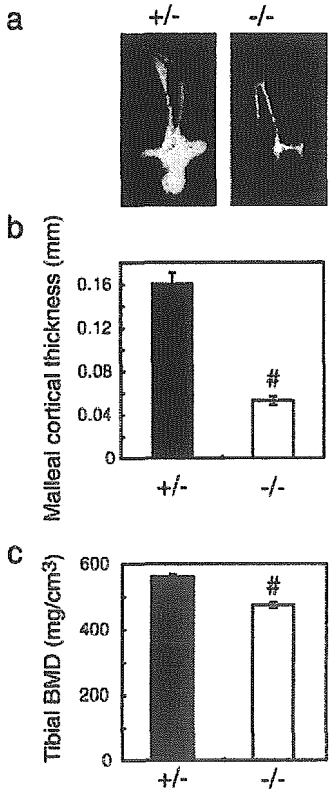

Fig. 3. Radiographical analysis of auditory ossicles and tibia. (a) Representative μCT images of the malleus from 8-week-old mice (n = 5 for +/− and n = 5 for −/−). (b) Malleal cortical thickness of mice described in panel a. (c) Tibial cortical BMD of mice described in panel a. $^{\#}P < 0.001$, versus heterozygous mice.

data suggest that osteoclastic bone resorption of auditory ossicles is elevated in the absence of OPG, leading to bone loss.

To test whether bone loss observed in $Opg^{-/-}$ mice is associated with differences in hearing ability, we assessed ABR thresholds at 6, 10, and 15 weeks of age in heterozygous and $Opg^{-/-}$ mice. ABR threshold was determined as the minimum sound pressure level (SPL) giving reproducible waveforms. At 6 weeks of age, the average ABR threshold of $Opg^{-/-}$ mice was similar to that of heterozygous littermate controls at frequencies from 2 to 20 kHz. However, at 10 weeks of age, $Opg^{-/-}$ mice began showing higher (i.e., worse) thresholds than controls (Fig. 4). By 15 weeks, the differences were even greater, with $Opg^{-/-}$ mice being more than 20 decibels (dB) less sensitive than heterozygous controls at the highest frequency of 20 kHz (Fig. 4). These data suggest that excessive bone remodeling can result in progressive hearing loss.

Discussion

In adult $Opg^{-/-}$ mice, we observed erosion of the malleus, incus, and stapes. Furthermore, TRAP activity was detected in all the three ossicles and the otic capsule of $Opg^{-/-}$ mice, indicating that osteoclastic bone resorption of auditory ossicles is elevated. It is unclear whether certain specific areas within each ossicle are preferentially resorbed or not. We also observed that $Opg^{-/-}$ mice show progressive hearing loss. The precise mechanisms of hearing loss in these mice are currently unknown. Since hearing loss in each animal was progressive, sudden loss of articulation between auditory ossicles is not likely to be the cause of impairment. We observed extensive resorption

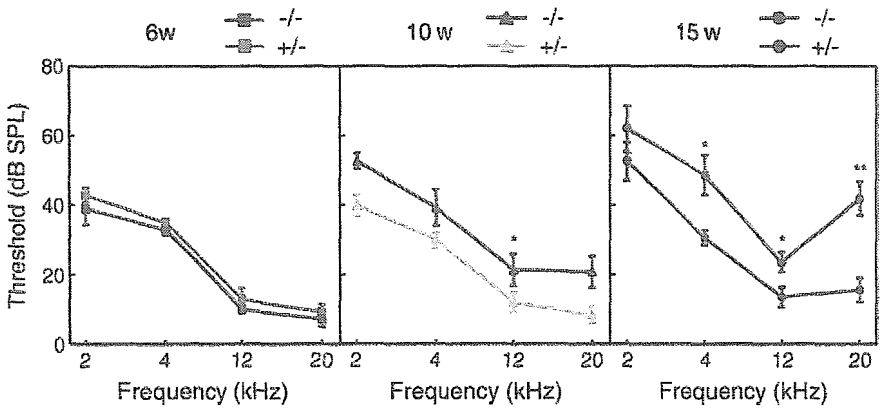

Fig. 4. Progressive increase in ABR thresholds of *Opg* $^{-/-}$ mice. Data points for thresholds at 2, 4, 12, and 20 kHz in *Opg* $^{-/-}$ mice and heterozygous controls at the ages of 6 (n = 5 each), 10 (n = 7 each), and 15 (n = 7 each) weeks. Significant differences between 15-week-old *Opg* $^{-/-}$ and heterozygous control mice are indicated with asterisks (*P < 0.05, **P < 0.01).

of the malleal processus brevis in *Opg*$^{-/-}$ mice, but the malleal processus brevis is dispensable for hearing function [2]. In *Opg*$^{-/-}$ mice, we observed that stapedial fixation, namely, the ligaments between the stapes and the otic capsule, was replaced with bone tissue. Among the observed morphological alterations including thinning of the malleal manubrium and incus body, stapedial fixation is the most likely cause of hearing loss in *Opg*$^{-/-}$ mice. Clinically, hearing loss in otosclerosis can be cured by surgical intervention at the stapedial–cochlear junction, indicating the importance of this junction in hearing.

OPG deficiency has been found in patients with juvenile Paget's disease, which is also known as idiopathic hyperphosphatasia [23–27] and characterized by markedly increased bone turnover. Paget disease of bone is a distinct and much more common disease than juvenile Paget's disease, characterized by excessive osteoclastic bone resorption followed by compensatory increase in osteoblastic bone formation [28]. Curiously, hearing is affected in approximately 50% of cases of Paget disease of bone involving the skull [29]. Hearing loss in patients with otosclerosis and Paget disease of bone could be due to the increased bone formation, which narrows the internal auditory canal and causes nerve atrophy. On the other hand, hearing loss has been positively correlated with loss of bone density in the otic capsule [30, 31]. Similarly, activating mutations in *TNFRSF11A*, which encodes RANK, cause expansile skeletal hyperphosphatasia, which features deafness in infancy or early childhood [32]. Familial expansile osteolysis, which is also caused by mutation in *TNFRSF11A* [33], is also associated with deafness.

Recent reports show that OPG is highly expressed in cochlear soft tissues and secreted into the perilymph and surrounding bone [34]. Furthermore, OPG levels increase with age in women [35–37]. The apparent lack of association between osteoporosis and hearing loss in humans [18] implies that the auditory ossicles and the otic capsule may be protected from osteoclastic bone resorption by OPG even in patients with postmenopausal and age-related osteoporosis. In conclusion, these data reveal a critical role for OPG as an "audioprotegerin" in maintaining quality of bone conduction by protecting auditory ossicles and the otic capsule from bone resorption. Impaired production of OPG in the temporal bone may be a risk factor for hearing loss.

Acknowledgments

We thank Shumpei Niida, Kyoji Ikeda, and Minako Sato for helpful discussions and Neelanjan Ray and Elise Lamar for critical reading of the manuscript. This work is supported by Grant-in-Aid for Young Scientists B (17791198 to SK) and Grant-in-Aid for Scientific Research B (17390420 to KM) from JSPS, and a Keio University Special Grant-in-Aid for Innovative Collaborative Research Projects.

References

[1] Mallo M. Formation of the middle ear: recent progress on the developmental and molecular mechanisms. Dev Biol 2001;231:410–9.
[2] Zhang Z, Zhang X, Avniel WA, Song Y, Jones SM, Jones TA, et al. Malleal processus brevis is dispensable for normal hearing in mice. Dev Dyn 2003;227:69–77.
[3] Teitelbaum SL, Ross FP. Genetic regulation of osteoclast development and function. Nat Rev Genet 2003;4:638–49.
[4] Karsenty G, Wagner EF. Reaching a genetic and molecular understanding of skeletal development. Dev Cell 2002;2:389–406.
[5] Franzoso G, Carlson L, Xing L, Poljak L, Shores EW, Brown KD, et al. Requirement for NF-κB in osteoclast and B-cell development. Genes Dev 1997;11:3482–96.
[6] Grigoriadis AE, Wang ZQ, Cecchini MG, Hofstetter W, Felix R, Fleisch HA, et al. c-Fos: a key regulator of osteoclast-macrophage lineage determination and bone remodeling. Science 1994;266:443–8.
[7] Matsuo K, Owens JM, Tonko M, Elliott C, Chambers TJ, Wagner EF. *Fosl1* is a transcriptional target of c-Fos during osteoclast differentiation. Nat Genet 2000;24:184–7.
[8] Takayanagi H, Kim S, Koga T, Nishina H, Isshiki M, Yoshida H, et al. Induction and activation of the transcription factor NFATc1 (NFAT2) integrate RANKL signaling in terminal differentiation of osteoclasts. Dev Cell 2002;3:889–901.
[9] Matsuo K, Galson DL, Zhao C, Peng L, Laplace C, Wang KZ, et al. Nuclear factor of activated T-cells (NFAT) rescues osteoclastogenesis in precursors lacking c-Fos. J Biol Chem 2004;279:26475–80.
[10] Simonet WS, Lacey DL, Dunstan CR, Kelley M, Chang MS, Luthy R, et al. Osteoprotegerin: a novel secreted protein involved in the regulation of bone density. Cell 1997;89:309–19.

[11] Yasuda H, Shima N, Nakagawa N, Yamaguchi K, Kinosaki M, Mochizuki S, et al. Osteoclast differentiation factor is a ligand for osteoprotegerin/osteoclastogenesis-inhibitory factor and is identical to TRANCE/RANKL. Proc Natl Acad Sci U S A 1998;95:3597–602.
[12] Martin TJ, Sims NA. Osteoclast-derived activity in the coupling of bone formation to resorption. Trends Mol Med 2005;11:76–81.
[13] Cooper C. Epidemiology of osteoporosis. Primer on the Metabolic Bone Diseases and Disorders of Mineral Metabolism. The American Society for Bone and Mineral Research; 2003. p. 307–13.
[14] Adams PF, Benson V. Current estimates from the National Health Interview Survey, 1991. Vital Health Stat 1992;10:1–232.
[15] Henkin RI, Lifschitz MD, Larson AL. Hearing loss in patients with osteoporosis and Paget's disease of bone. Am J Med Sci 1972;263:383–92.
[16] Haboubi NY, Hudson PR. Factors associated with Colles' fracture in the elderly. Gerontology 1991;37:335–8.
[17] Clark K, Sowers MR, Wallace RB, Jannausch ML, Lemke J, Anderson CV. Age-related hearing loss and bone mass in a population of rural women aged 60 to 85 years. Ann Epidemiol 1995;5:8–14.
[18] Helzner EP, Cauley JA, Pratt SR, Wisniewski SR, Talbott EO, Zmuda JM, et al. Hearing sensitivity and bone mineral density in older adults: the Health Aging and Body Composition Study. Osteoporos Int 2005;16:1675–82.
[19] Bucay N, Sarosi I, Dunstan CR, Morony S, Tarpley J, Capparelli C, et al. *Osteoprotegerin*-deficient mice develop early onset osteoporosis and arterial calcification. Genes Dev 1998;12:1260–8.
[20] Mizuno A, Amizuka N, Irie K, Murakami A, Fujise N, Kanno T, et al. Severe osteoporosis in mice lacking osteoclastogenesis inhibitory factor/osteoprotegerin. Biochem Biophys Res Commun 1998;247:610–5.
[21] Amizuka N, Shimomura J, Li M, Seki Y, Oda K, Henderson JE, et al. Defective bone remodelling in osteoprotegerin-deficient mice. J Electron Microsc (Tokyo) 2003;52:503–13.
[22] Nakamura M, Udagawa N, Matsuura S, Mogi M, Nakamura H, Horiuchi H, et al. Osteoprotegerin regulates bone formation through a coupling mechanism with bone resorption. Endocrinology 2003;144:5441–9.
[23] Cundy T, Hegde M, Naot D, Chong B, King A, Wallace R, et al. A mutation in the gene *TNFRSF11B* encoding osteoprotegerin causes an idiopathic hyperphosphatasia phenotype. Hum Mol Genet 2002;11:2119–27.
[24] Whyte MP, Obrecht SE, Finnegan PM, Jones JL, Podgornik MN, McAlister WH, et al. Osteoprotegerin deficiency and juvenile Paget's disease. N Engl J Med 2002;347:175–84.
[25] Chong B, Hegde M, Fawkner M, Simonet S, Cassinelli H, Coker M, et al. Idiopathic hyperphosphatasia and *TNFRSF11B* mutations: relationships between phenotype and genotype. J Bone Miner Res 2003;18:2095–104.
[26] Janssens K, de Vernejoul MC, de Freitas F, Vanhoenacker F, Van Hul W. An intermediate form of juvenile Paget's disease caused by a truncating *TNFRSF11B* mutation. Bone 2005;36:542–8.
[27] Cundy T, Davidson J, Rutland MD, Stewart C, DePaoli AM. Recombinant osteoprotegerin for juvenile Paget's disease. N Engl J Med 2005;353:918–23.
[28] Roodman GD, Windle JJ. Paget disease of bone. J Clin Invest 2005;115:200–8.
[29] Teufert KB, Linthicum Jr F. Paget disease and sensorineural hearing loss associated with spiral ligament degeneration. Otol Neurotol 2005;26:387–91.
[30] Huizing EH, de Groot JA. Densitometry of the cochlear capsule and correlation between bone density loss and bone conduction hearing loss in otosclerosis. Acta Otolaryngol 1987;103:464–8.
[31] Monsell EM. The mechanism of hearing loss in Paget's disease of bone. Laryngoscope 2004;114:598–606.
[32] Whyte MP, Hughes AE. Expansile skeletal hyperphosphatasia is caused by a 15-base pair tandem duplication in *TNFRSF11A* encoding RANK and is allelic to familial expansile osteolysis. J Bone Miner Res 2002;17:26–9.
[33] Hughes AE, Ralston SH, Marken J, Bell C, MacPherson H, Wallace RG, et al. Mutations in *TNFRSF11A*, affecting the signal peptide of RANK, cause familial expansile osteolysis. Nat Genet 2000;24:45–8.
[34] Zehnder AF, Kristiansen AG, Adams JC, Merchant SN, McKenna MJ. Osteoprotegerin in the inner ear may inhibit bone remodeling in the otic capsule. Laryngoscope 2005;115:172–7.
[35] Yano K, Tsuda E, Washida N, Kobayashi F, Goto M, Harada A, et al. Immunological characterization of circulating osteoprotegerin/osteoclastogenesis inhibitory factor: increased serum concentrations in postmenopausal women with osteoporosis. J Bone Miner Res 1999;14:518–27.
[36] Browner WS, Lui LY, Cummings SR. Associations of serum osteoprotegerin levels with diabetes, stroke, bone density, fractures, and mortality in elderly women. J Clin Endocrinol Metab 2001;86:631–7.
[37] Ueland T, Brixen K, Mosekilde L, Mosekilde L, Flyvbjerg A, Bollerslev J. Age-related changes in cortical bone content of insulin-like growth factor binding protein (IGFBP)-3, IGFBP-5, osteoprotegerin, and calcium in postmenopausal osteoporosis: a cross-sectional study. J Clin Endocrinol Metab 2003;88:1014–8.

BRAIN RESEARCH 1068 (2006) 237–247

available at www.sciencedirect.com

SCIENCE DIRECT®

www.elsevier.com/locate/brainres

BRAIN RESEARCH

Research Report

Nuclear factor-kappa B nuclear translocation in the cochlea of mice following acoustic overstimulation

Masatsugu Masuda[a,*], Reiko Nagashima[b], Sho Kanzaki[a], Masato Fujioka[a], Kiyokazu Ogita[b], Kaoru Ogawa[a]

[a]Department of Otolaryngology, School of Medicine, Keio University, 35 Shinanomachi, Shinjuku-ku, Tokyo 160-8582, Japan
[b]Department of Pharmacology, Setsunan University, 45-1 Nagaotoge-cho, Hirakata, Osaka 573-0101, Japan

ARTICLE INFO

Article history:
Accepted 2 November 2005
Available online 22 December 2005

Theme:
Sensory systems
Topic:
Auditory, vestibular, and lateral line: periphery

Keywords:
Cochlea
Inducible nitric oxide
Lateral wall
Noise trauma
Nuclear factor-kappa B
p65

ABSTRACT

There is increasing evidence to suggest that the expression of many molecules in the lateral wall of the cochlea plays an important role in noise-induced stress responses. In this study, activation of the nuclear transcription factor nuclear factor-kappa B (NF-κB) was investigated in the cochlea of mice treated with intense noise exposure (4 kHz, octave band, 124 dB, for 2 h). The present noise exposure led to remarkable auditory brainstem response threshold shifts and cochlear damage on surface preparations. To assess the effects of noise exposure on NF-κB/DNA binding activity in the cochlea, we prepared nuclear extracts from the cochlea at different time points after noise exposure and carried out an electrophoretic mobility shift assay using a probe specific to NF-κB. NF-κB/DNA binding was significantly enhanced in the cochlea 2–6 h after noise exposure and returned to basal levels after 12 h. Supershift analysis using antibodies against p65 and p50 proteins, which are components of NF-κB, demonstrated that enhancement of NF-κB/DNA binding was at least in part due to nuclear translocation of p65. An immunohistochemical study also showed that nuclear translocation of both p65 and p50 was observed in the lateral wall after noise exposure and that there may be a possible close association between p65 and enhanced inducible nitric oxide synthase expression. These results suggest that NF-κB may have a detrimental role in the response to acoustic overstimulation in the cochlea of mice.

* *Corresponding author.* Fax: +81 3 5379 0335.
E-mail address: masu13@sc.itc.keio.ac.jp (M. Masuda).

0006-8993/$ – see front matter © 2005 Elsevier B.V. All rights reserved.
doi:10.1016/j.brainres.2005.11.020

Abbreviations:
ABR, auditory brainstem response
AP-1, activator protein-1
Ca^{2+}, calcium
EAA, excitory amino acid
EMSA, electrophoretic mobility shift assay
IHC, inner hair cell
iNOS, inducible nitric oxide synthase
K^+, potassium
NF-κB, nuclear factor-kappa B
NO, nitric oxide
OC, organ of Corti
OHC, outer hair cell
PBS, phosphate-buffered saline
PFA, paraformaldehyde
PI, propidium iodide
ROS, reactive oxygen species
SPL, sound pressure level

1. Introduction

Intense noise exposure can lead to permanent damage to the sensory epithelium, the organ of Corti (OC), which includes sensory cells like the inner hair cells (IHCs) and outer hair cells (OHCs). The mechanisms of noise trauma are as follows: generation of nitric oxide (NO) or reactive oxygen species (ROS) leading to cytotoxicity to the sensory cells (Yamane et al., 1995; Ohlemiller et al., 1999; Ohinata et al., 2000; Nakashima et al., 2003; Shi and Nuttall, 2003); calcium (Ca^{2+}), potassium (K^+), and excitatory amino acid (EAA) overload leading to damage of sensory cells (Bohne and Rabbitt, 1983; Hsu et al., 2000; Jager et al., 2000; Hirose and Liberman, 2003; Hsu et al., 2004); and degeneration of the cochlear cells (Bohne and Rabbitt, 1983; Jager et al., 2000; Wang et al., 2002; Hirose and Liberman, 2003). There is a variety of evidence that the lateral wall, consisting of the spiral ligament and the stria vascularis, plays a critical role in these mechanisms.

Since a variety of stress responses occur, it is possible that simultaneous modulation of multiple mechanisms instead of a single mechanism can lead to better treatment outcomes for the hearing impairment resulting from noise trauma. This may be provided by modulation of transcription factors because one transcription factor regulates the expression of many genes in response to a single stimulus that induces tissue damage.

One of the most notable rapidly inducible transcription factors is nuclear factor-kappa B (NF-κB). NF-κB is composed of homo- and hetero-dimeric complexes of Rel family proteins including p65, p50, c-Rel, p52, and RelB. A hetero-dimer of p50/p65 is the predominant form of NF-κB (Bowie and O'Neill, 2000), however, a homodimer of p65/p65 or p50/p50 also exists (Ghosh et al., 1998). NF-κB exists in a latent form in the cytoplasm of unstimulated cells and is comprised of a transcriptionally active dimer bound to an inhibitor protein. Diverse stimulants lead to degradation of the NF-κB inhibitory protein and activation of NF-κB. The activated NF-κB dimer can then translocate into the nucleus and activate target genes by binding with high affinity to κB elements at their promoters. NF-κB plays a pivotal role in immune and inflammatory responses (Sha, 1998; Denk et al., 2000), neuronal development, neuronal cell death and survival, and neurodegeneration (Wooten, 1999; Denk et al., 2000; Mattson et al., 2000a,b).

Since activation of NF-κB induces both cytoprotective and cytotoxic proteins, the role of NF-κB in the mammalian cochlea has not been clearly determined. Jiang et al. reported that NF-κB protected murine cochlear hair cells from aminoglycoside-induced ototoxicity (Jiang et al., 2005). Ramkumar et al. suggested that NF-κB might protect the chinchilla cochlea from noise trauma because activation of NF-κB occurred in a similar time frame as the peak expression of the A1 adenosine receptor which acted in a protective role for the noise-exposed cochlea (Ramkumar et al., 2004). On the other hand, Merchant et al. suggested that human idiopathic sudden sensorineural hearing loss might be the result of abnormal activation of cellular stress pathways involving NF-κB (Merchant et al., 2005). Watanabe et al. suggested that apoptosis of cochlear cells was triggered by inducible nitric oxide synthase (iNOS)

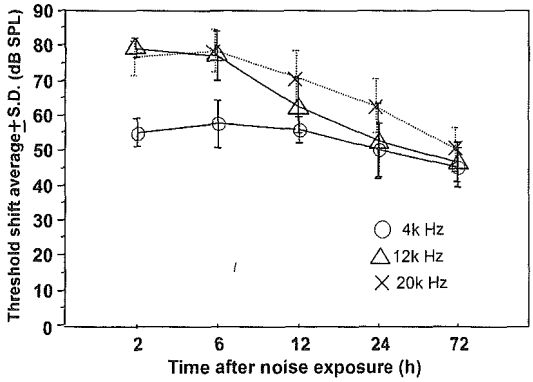

Fig. 1 – Changes in ABR thresholds after noise exposure with 124 dB SPL octave band noise, centered at 4 kHz, for 2 h of noise exposure. The graph shows remarkable ABR threshold elevations at the frequencies of 4, 12, and 20 kHz.

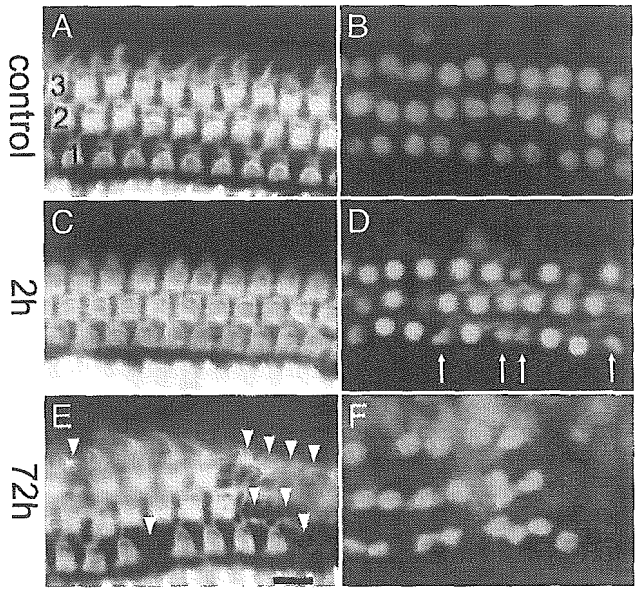

Fig. 2 – Surface preparations were obtained to confirm the cochlear damage. Flourescein phalloidin staining (A, C, E) was used to outline the OHCs. PI staining (B, D, F) was used to observe nuclear morphological change. (A, B) Preparations in the untreated mouse around the area of 50% of the distance from the apex to the base of the OC which is the area known to correspond to 10 kHz. These preparations show the regular outline of three rows of OHCs (A) and normal nuclear morphology (B). (C, D) Preparations in the mouse 2 h after noise exposure around the area of 50% of the distance of the OC. These preparations demonstrate the normal outlines of the OHCs (C), however, some nuclei have morphological changes (arrows in D) indicating damaged cells, even further away than 25%, which is the area known to correspond to 4 kHz, at only 2 h after noise exposure. (E, F) Preparations around the area of 25% of the OC of the mouse 72 h after noise exposure. They show loss of OHCs (E, arrow heads) and much more nuclear morphological changes than at 2 h after exposure. Scale bar = 10 μm.

through activation of NF-κB in cisplatin-treated mice (Watanabe et al., 2002). It was also reported that excess expression of iNOS followed by increased NO-related ROS contributes to noise-induced hearing loss (Shi and Nuttall, 2003; Shi et al., 2002, 2003; Ohinata et al., 2003). Therefore, there is also the possibility that NF-κB acts in a ototoxic role in noise trauma through the induction of enhanced iNOS expression. It has been shown that NF-κB was activated in the chinchilla cochlea after noise exposure (Ramkumar et al., 2004), however, the temporal and spatial aspects of activation were not evaluated. These aspects are important for transcription factors because their downstream targets may be stimulus-, temporal-, structure-, or cell type-specific. Activator protein-1 (AP-1), another notable transcription factor, is a very impressive example of this importance. Enhancement of AP-1/DNA binding activity 5 h after noise exposure is protective in the OC and the lateral wall, however, it is cytotoxic in the OC 15 h after exposure (Matsunobu et al., 2004). AP-1 activity is regulated by NF-κB (Fujioka et al., 2004), and activation of NF-κB and AP-1 leads to the coordinated expression of target genes (Rahman et al., 2004).

Therefore, we examined the time course of NF-κB activation with an electrophoretic mobility shift assay (EMSA), cellular localization, and immunohistochemistry to examine the possible association between NF-κB activation and induction of enhanced iNOS expression.

2. Results

2.1. *Auditory brainstem response threshold shift and surface preparation*

Cochlear damage was examined functionally by auditory brainstem responses (ABRs) and morphologically by surface preparations. The noise, 124 dB sound pressure level (SPL) octave band noise, centered at 4 kHz for 2 h, produced profound ABR threshold shifts at the frequencies of 4, 12, and 20 kHz from 2 h to 72 h after noise exposure (Fig. 1).

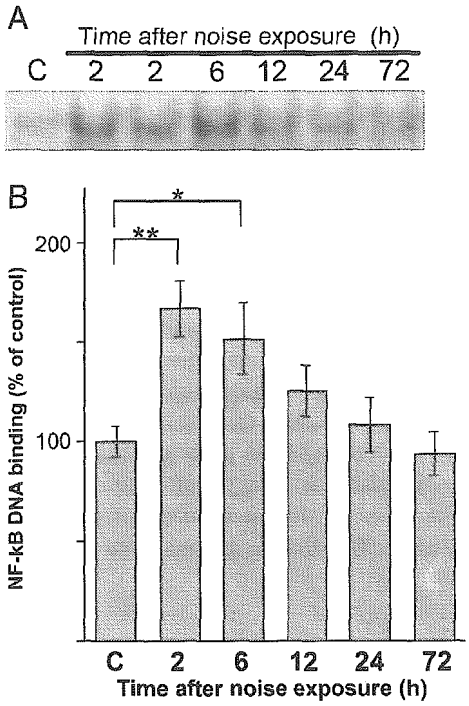

Fig. 3 – Time course of NF-κB/DNA binding activity after noise exposure. (A) NF-κB binding was analyzed by an EMSA as described in the text. The cochleae were processed after the resting times indicated on the figure (C, control). Bound probes are more intense in the cochleae 2–6 h after noise exposure than in the untreated cochleae and are less intense after 6 h. (B) Densitometric data. Autoradiograms were quantified by scanning with the NIH imaging software, and binding activities were normalized to the value prior to noise exposure. Values are expressed as the percent of the value prior to exposure; numbers are mean ± SE. **, * Significantly different from pre-exposure levels ($P < 0.01$ and *$P < 0.05$ by unpaired t test).**

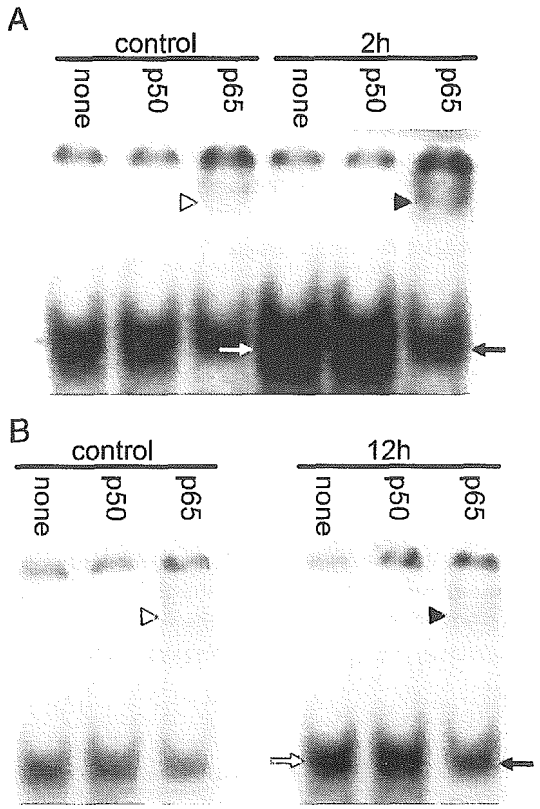

Fig. 4 – Supershift analysis of NF-κB/DNA binding. (A) Analysis of 2 h after noise exposure. (B) Analysis of 12 h after noise exposure. After incubation for NF-κB/DNA binding, the reaction mixture was further incubated for 16 h at 4 °C in the absence (none) or presence of 3 μg anti-p65 (p65) or anti-p50 (p50) antibody as described in the text. Migration of the probe/protein complex (black arrows and white arrows) is partially retarded (black arrow heads and white arrow heads) in the cochlea tissue after incubation with anti-p65 antibody. The supershifted band is more intense 2 h (A, black arrow head) after noise exposure than 12 h (B, black arrow head). The bands of the NF-κB/DNA probe not bound with antibody are also more intense in mice 2 h after noise exposure (white arrows) than those of untreated mice and of mice 12 h after noise exposure. This finding is consistent with the EMSA results.

The surface preparation from the untreated mouse showed a normal OHC outline (Fig. 2A) and a normal nucleus (Fig. 2B). Few OHC losses were observed in the cochlea 2 h after noise exposure (Fig. 2C), however, shrunken nuclear bodies, which indicated dying hair cells (Hu et al., 2002; Minami et al., 2004), were observed (Fig. 2D, arrows). The observed area was about 50% of the distance from the apex to the base where the OC was maximally vibrated by the 10 kHz tone (Ou et al., 2000). The morphological changes around the area of 50% of the distance were the same as the area of 25%, where the OC was maximally vibrated by the 4 kHz tone, 2 h after noise exposure. The cochlea was damaged even if the observed area was 50% of the distance from the apex, where the OC was not maximally vibrated by 4 kHz tone, 2 h after noise exposure. Seventy-two hours after the noise exposure, OHC losses were clearly observed around the area of 25% (Fig. 2E, arrow heads) and greater than 70% (data not shown) of the distance from the apex, and more shrunken nuclear bodies were observed than 2 h of noise exposure (Fig. 2F). The damage of the IHC was not found at any time point.

2.2. *Effects of noise exposure on NF-κB/DNA binding*

Nuclear extracts of the whole cochlea demonstrated binding of endogenous NF-κB to the radiolabeled oligonucleotide probe (Fig. 3A). Several control experiments confirmed the specificity of the observed binding. Gels showed no band in the absence of nuclear extracts or in the presence of excessive non-radioactive oligonucleotides probe. In contrast, the addition of an unlabeled double-stranded oligonucleotide probe lacking the consensus core element for NF-κB did not inhibit the binding of NF-κB (data not shown).

Binding activity was determined at various times up to 72 h after noise exposure in nuclear extracts of the cochlea (Figs. 3A, B). A clear elevation of the NF-κB/DNA binding activity was observed in the cochlea. Binding activity was significantly elevated about 1.7-fold 2 h after noise exposure and remained significantly elevated until 6 h after noise exposure and returned to near baseline levels 12 h after noise exposure.

2.3. *Protein composition of the NF-κB complex*

In order to evaluate the participation of NF-κB family proteins in NF-κB/DNA binding, nuclear extracts were individually incubated with antibodies against p65 and p50 prior to the incubation with the radiolabeled DNA probe. Because the highest increase in NF-κB/DNA binding was observed 2 h after noise exposure, this time point was selected for analysis. The time point of 12 h was also selected to confirm that the supershifted band would also return to near baseline levels and to confirm the result of the EMSA. Protein/antibody complexes bound to the DNA probe will shift the position of the complex on the gel to a higher molecular size, i.e. slower migration. Such a "supershift" was observed for p65 (Fig. 4, black arrow heads and white arrow heads), and the difference of the band intensity between untreated mice (Fig. 4, white arrow head) and noise-exposed mice (Fig. 4 black arrow head) was more clear after 2 h (Fig. 4A) than 12 h (Fig. 4B). The bands of NF-κB/DNA probe complexes of p65 were less intense (Fig. 4, black arrows) than those without antibodies (none in Fig. 4) and with an antibody for p50 (Fig. 4, white arrows) because a part of the complexes of p65 has translocated to the supershifted bands (Fig. 4, black arrow heads and white arrow heads).

When the hippocampal nuclear extracts were used as a sample in the supershift analysis, NF-κB/DNA binding was completely inhibited by the addition of anti-p50 antibody (data not shown). This meant that the anti-p50 antibody used in the present study was validated. In the case of the cochlea, however, binding of p50 was not significantly affected by preincubation with this antibody. These findings suggest that p65 is a major protein component of the NF-κB complex for DNA binding in untreated mice, whereas p50 is not. Following the 2 h of noise exposure, the p65 supershift was also evident, and the p50 supershift was not affected by the preincubation with the antibodies. Therefore, p65 may be a major component of the NF-κB binding activity following noise exposure.

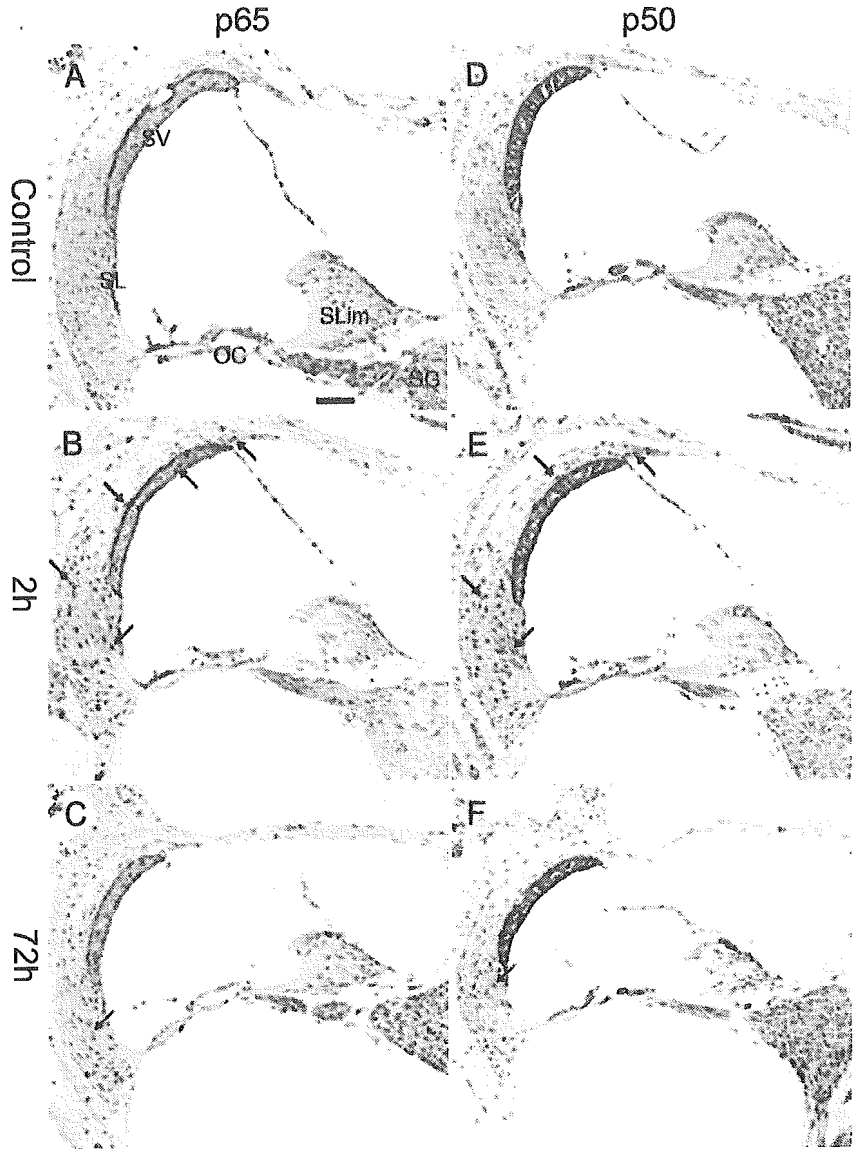

Fig. 5 – Comparison of immunolocalization of NF-κB in mid-modiolar sections in the cochlea of untreated mice (A, D) versus mice 2 h (B, E) and 72 h (C, F) after noise exposure. These sections were taken from the middle turn of the cochleae. There were no remarkable differences in the immunohistochemical staining pattern among the apical, middle, and basal turns. (A–C) Immunostaining for p65. (D–F) Immunostaining for p50. The cells of the lateral wall have darkly stained nuclei 2 h after noise exposure (arrows), indicative of NF-κB activation. On the other hand, the nuclei are not stained before noise exposure and become less intensely stained 72 h after noise exposure. The positive stain of the cytoplasm indicates the latent form of NF-κB. Scale bar = 50 μm. Scale bar applies to A–F.

The difference of the band intensity of NF-κB/DNA probe complex between untreated mice and noise-exposed mice was more clear after 2 h (Fig. 4A, white arrows) than after 12 h (Fig. 4B, white arrows). This was consistent with the EMSA results.

2.4. *p65 and p50 immunostaining in the cochlea*

Figs. 5 and 6 show immunolocalization of p65 (Figs. 5A–C, 6) and p50 (Figs. 5D–F) in mouse cochlea 2 h (Figs. 5B, E, 6) and 72 h (Figs. 5C, F) after noise exposure and in the unexposed cochlea (Figs. 5A, D). There was little or no nuclear immunostaining for p65 and p50 in the unexposed cochlea. On the other hand, prominent nuclear localization of these antibodies occurred in the lateral wall 2 h after noise exposure (Figs. 5B, E), and then the nuclear immunostaining became much less intense 72 h after (Figs. 5C, F). Immunostaining translocations from the cytoplasms in untreated mice into the nuclei of noise-exposed mice for p65 were seen in cells of the spiral ligament and of the stria vascularis. As for p50, the translocation was seen in the spiral ligament but was not clearly seen in the stria vascularis. Cytoplasm immunostaining with these antibodies was found in the cells of the OC (Fig. 6), the spiral limbus, and the spiral ganglion (Fig. 5) in both the noise-exposed and the untreated cochlea, although the clear immunostaining shift from the cytoplasm into the nucleus did not occur in noise-exposed cochlea. Along the cochlear spiral, the

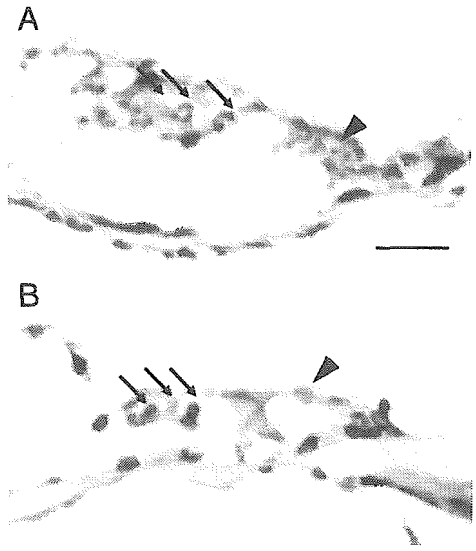

Fig. 6 – Comparison of immunolocalization of p65 in the OC between the apical turn (A) and the middle turn (B) 2 h after noise exposure. Along the cochlear spiral and the lateral wall, the immunostaining pattern of the OC was homogeneous. There was no difference in the immunohistochemical staining pattern of p65 and p50 in the OC at any time point. Arrow, OHC; arrow head, IHC. Scale bar = 20 μm. The scale bar applies to A and B.

immunostaining pattern of the lateral wall was homogeneous from the apex to the base. This homogenous pattern was also seen in the other parts, including the OC (Fig. 6). Both the OC of the apical turn (Fig. 6A) and the middle turn (Fig. 6B) lacked nuclear immunostaining for p65 after noise exposure. There was no difference in the immunohistochemical staining pattern of the OC with either p65 or p50. When the primary antibody was omitted, no staining was observed in the noise-exposed cochlea (data not shown).

The remarkable morphological differences in the lateral wall tissue of the slides from the different time points were not seen.

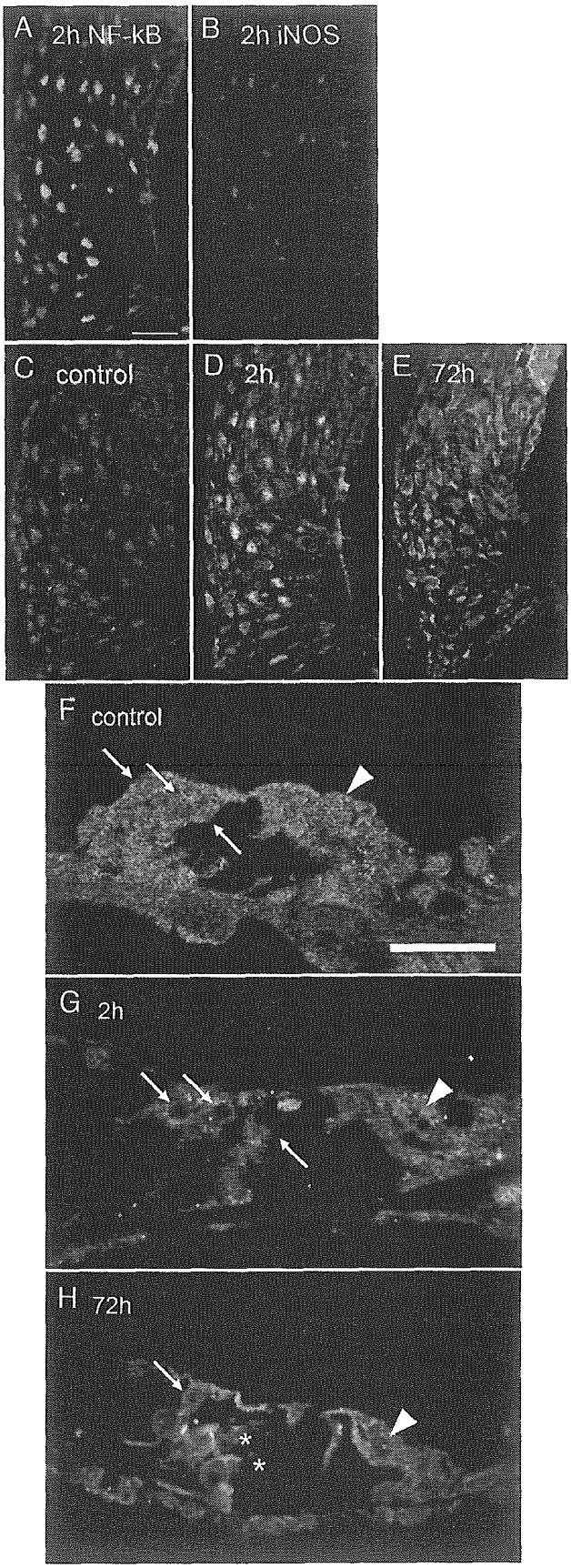

Fig. 7 – Double labeling immunohistochemistry was used to observe the relationship between NF-κB activation (A) and iNOS production (B) in the NF-κB activated cells of the lateral wall (A–E) and the cells of the OC (F–H). (C–H) Merged images of NF-κB (green) and iNOS (red). The sections were taken from the middle turn. There was no remarkable difference in the immunohistochemical staining pattern among the apical, middle, and basal turns. Most of the cells that had positive nuclear staining for p65, which is indicative of NF-κB activation, also stained positive for iNOS (D, yellow) in the mice 2 h after noise exposure. Double labeled cells (yellow) were not seen in the untreated mice (C), and weak double immunoreactivity in the cytoplasm was seen in the mice 72 h after noise exposure (E). In the OC, p65 immunolocalized (green or yellow) to the cytoplasm, and there was no clear immunolocalization shift into the nuclei of sensory cells, which consisted of IHCs (arrows) and OHCs (arrow heads) and other cells of the OC at 2 h (G) and at 72 h (H) after noise exposure. Damaged OHCs are observed (*). Scale bar = 25 μm. The scale bar in figure A applies to A–E. The scale bar in figure F applies to F–H.

2.5. iNOS immunoreactivity in the p65 activated cells

The supershift analysis revealed that a major component of the NF-κB binding activity following noise exposure was p65, and the immunohistochemical study revealed that the activation was prominent in the spiral ligament of the lateral wall. Therefore, a double labeling immunohistochemical study for p65 and iNOS in the spiral ligament was conducted to explore the possibility that NF-κB regulated iNOS expression in the noise-exposed cochlea.

In the lateral wall of mice 2 h after noise exposure, most of the NF-κB activated cells, which demonstrated nuclear immunostaining for p65 (Fig. 7A, green), also showed positive immunostaining for iNOS (Fig. 7B, red). Furthermore, the colocalization of p65 and iNOS was observed as strong yellow nuclear immunostaining in the merged image (Fig. 7D). In the lateral wall of untreated mice, no significant colocalization was observed (Fig. 7C). In the lateral wall of mice 72 h after noise exposure, weak colocalization was observed in the cytoplasm (Fig. 7E).

In the OC, no nuclear staining for p65 or iNOS was observed at any time point (Figs. 7F–H). These sections were from the middle turn of the cochleae. There were no remarkable differences in the immunohistochemical staining pattern in the apical, middle, and basal turns. When the primary antibody was omitted, no staining was observed in the noise-exposed cochlea (data not shown).

3. Discussion

The present study provides evidence that NF-κB/DNA binding in the mammalian cochlea is increased, with a peak level around 2 h after the end of the noise exposure, and indicates that there is a possible close association between NF-κB activation and iNOS expression following noise overstimulation.

The present noise condition resulted in noise-induced cochlear damage. It was confirmed by functional (Fig. 1) and histological (Fig. 2) studies with ABR and surface preparations respectively. The damage of the cochlea occurred throughout the area of greater than 25% of the distance from the apex to the base. The present distribution of OHC losses and/or nuclear condensation at 2 h after noise exposure was consistent with previous studies on noise-induced cellular injury in the mammalian cochlea (Hu et al., 2002; Wang et al., 2002; Minami et al., 2004). Since the present condition damaged the wide range of cochlear spiral, the immunostaining pattern was homogenous throughout the cochlea. Under this noise condition, the results of the immunohistochemical staining suggested a marked elevation of NF-κB/DNA binding in the lateral wall tissues, while no significant changes were observed in the OC and the spiral ganglion.

NF-κB is activated by oxidative stress, thereby acting as a "stress sensor" (Mattson et al., 2000a). The lateral wall is critical for normal functioning of the cochlea and for many pathologies including noise trauma, although the lateral wall is not a sensory epithelium like the OC. Examples of the crucial roles of the lateral wall are activation of a transcription factor such as AP-1 (Ogita et al., 2000; Shizuki et al., 2002; Matsunobu et al., 2004); generation of NO and ROS (Yamane et al., 1995; Ohinata et al., 2000; Takumida and Anniko, 2001; Nakashima et al., 2003; Ohinata et al., 2003; Shi and Nuttall, 2003); production of antioxidant enzymes (Jacono et al., 1998; Yamasoba et al., 1998; Ohlemiller et al., 1999); clearance of EAA (Li et al., 1994); and maintenance of electrochemical homeostasis (Spicer and Schulte, 1996; Hsu et al., 2000; Ichimiya et al., 2000; Kikuchi et al., 2000; Suko et al., 2000; Hsu et al., 2004). The lateral wall tissues may increase metabolic activity to maintain the above functions. There is compelling evidence that the lateral wall normally does not sustain permanent damage, however, their transiently increased metabolic activity might result in formation of free radicals after noise exposure (Yamane et al., 1995). Since NF-κB is a redox-sensitive transcription factor like AP-1 and acts as a "stress sensor" (Mattson et al., 2000a), the oxidative stress in the lateral wall may lead to NF-κB activation. The lateral wall responses mentioned above and NF-κB activation showed in the present study are also temporally consistent because the responses in the lateral wall after noise overstimulation mentioned above were initiated during noise exposure or within a few hours after the end of noise exposure. The peak level of NF-κB activation also occurred in the same time frame as shown in the present study.

In addition to these close associations among NF-κB, noise trauma, and the lateral wall, the present study showed that NF-κB activated cells had increased iNOS expression (Fig. 7). Increased iNOS expression leads to excess NO production. Excess NO leads to the formation of peroxynitrite, a powerful oxidant. Finally, cell death may be initiated by many mechanisms, including lipid peroxidation, protein nitration, DNA damage, or the irreversible inhibition of respiration (Keynes and Garthwaite, 2004). It was suggested that the iNOS-dependent cell injury mechanisms were associated with noise-induced hearing loss (Ohinata et al., 2003; Shi and Nuttall, 2003; Shi et al., 2003). Since NO induced by iNOS readily permeates tissue and can diffuse hundreds of microns away from the source where it was generated (Pryor et al., 1997), the present NF-κB stimulating iNOS expression in the lateral wall can result in oxidative stress in the whole cochlea. This suggests a possible detrimental role of NF-κB in the whole cochlea after noise overstimulation. For example, there is evidence that glucocorticoids inhibit NF-κB mediated molecular expression and provide therapeutic effects for central nervous system disease, sepsis, myocardial disease, hepatitis, and rheumatic disease (Handel, 1997; Xu et al., 1998; D'Acquisto et al., 2002; Garside et al., 2004). As for the cochlea, glucocorticoid administration during or immediately after noise overstimulation has protective effects in the mammalian cochlea (Mori et al., 2004; Takemura et al., 2004; Wang and Liberman, 2002). These glucocorticoid effects indicate that NF-κB activation can damage the noise-exposed cochlea.

However, the lateral wall cells showed no remarkable morphological change with NF-κB activation though they had robust iNOS expression (Figs. 7C–E). On the other hand, the OC was damaged without NF-κB activation (Figs. 7F–H). Considering that NF-κB activated cells were not damaged, NF-κB might play a protective role in each cell level. This consideration is consistent with the protective role of NF-κB in aminoglycoside-induced ototoxicity (Jiang et al., 2005). OHC death of the murine

cochlea induced by aminoglycoside antibiotics is mediated by ROS and can be prevented by antioxidants. Jiang et al. showed that NF-κB was not activated in OHCs of aminoglycoside-treated mice without antioxidants, however, it was activated there by cotreatment with antioxidants.

We cannot fully explain why the IHC had no morphological change and no nuclear immunostaining for NF-κB. There must be NF-κB-independent cytoprotective and/or cytotoxic pathways after noise exposure, and the balance between NF-κB-dependent and -independent pathways must determine the degree of the noise trauma.

As mentioned above, the role of the transcription factor is structure or cell type-specific, therefore, evaluation of its spatial aspects, as in the present study, is very important. AP-1 was quantified in the OC, lateral wall, and spiral ganglion independently along the time course. There is evidence that AP-1 has differential roles in the OC and the lateral wall and even in the OC at different times (Ogita et al., 2000; Shizuki et al., 2002; Matsunobu et al., 2004). Therefore, future studies of NF-κB-related pathways must quantify several components of the NF-κB family.

Some of the staining pattern for iNOS was not consistent with previous reports. Our data showed iNOS expression in the spiral ligament. Watanabe et al. also showed NF-κB activation and iNOS expression in the lateral wall in cisplatin-treated mice (Watanabe et al., 2002), however, Shi et al. showed iNOS expression in the stria vascularis but not in the spiral ligament in the lateral wall after noise exposure (Shi et al., 2003). This dissimilar result could be due to different techniques employed and the noise condition. For example, we fixed the cochlea by local perfusion only; on the other hand, the others fixed with cardiac perfusion. Second, we and Watanabe et al. fixed the cochlea with 4% PFA overnight and used paraffin embedding; on the other hand, Shi et al. used surface preparation fixed with 4% PFA for 4 h. Third, the noise conditions were different. The noise used in the study by Shi et al. was 110 dB SPL broad band noise, 3 h/day, for three consecutive days. This was far different from our noise condition described in Experimental procedures.

The results of the supershift and immunohistochemistry analyses indicate that the increase in NF-κB/DNA binding in the lateral wall is, at least in part, due to enhanced activation of p65. Although densitometric data show no significant differences in NF-κB/DNA activity between 72 h after noise exposure and lack of exposure (Fig. 3B), immunohistochemical staining suggest that p65 may still work at this time point (Fig. 5C) to some degree.

The supershift analysis of p50 indicates that p50 is not a component of NF-κB in the noise-exposed mouse cochlea. However, there were intense nuclear immunoreactivities of p50 2 h after noise exposure and less intense nuclear immunoreactivities 72 h after noise exposure (Figs. 5E, F). There may be several reasons for the inconsistency between the EMSA data and the immunohistochemical studies for p50. It is possible that different homodimers like p65/p65 or p50/p50 are implicated in noise trauma. The p65/p65 homodimer can translocate into the nucleus and bind the κB element in the noise-exposed cochlea. On the other hand, p50/p50 can translocate into the nucleus, however, it cannot bind the κB element in the noise-exposed cochlea. Therefore, immunolocalization of p50 was shown in the nucleus; however, the supershifted band was not seen in the supershift assay. Nuclear immunostaining translocation from the cytoplasm into the nucleus for p65 was clearly seen in the stria vascularis; however, it was not seen for p50. This difference in immunoreactivity between p65 and p50 in the stria vascularis may come from the existence of different NF-κB dimers as mentioned above in the cochlea.

In summary, NF-κB has the potential to play a detrimental role in the noise-exposed cochlea through the expression of iNOS, and the activation of NF-κB in response to noise exposure selectively occurs in the lateral wall in the early time frame. On the other hand, it has the potential to play a protective role in each cell of the lateral wall. Therefore, further evaluations will be needed before NF-κB becomes a target of the treatment of noise-induced hearing loss.

4. Experimental procedures

4.1. *Experimental groups and experimental design*

Mice used in this study were male C57BL/6 J mice obtained from the Saitama-experimental animal center (Saitama, Japan) and entered into the study at 5 weeks of age. Cochlear function was tested in each animal via measurement of ABRs. Animals were randomly assigned to either a matrix of noise exposure or a control group receiving no noise exposure. First, we conducted an EMSA to investigate the activation of NF-κB/DNA binding in the mouse cochlea after noise exposure. Second, we conducted supershift analysis to analyze the composition of NF-κB proteins bound to the DNA probe. Third, we conducted immunohistochemistry to study the cellular localization of NF-κB and the relationship between NF-κB and iNOS in the mouse cochlea after noise exposure and in the cochlea unexposed to noise. For the EMSA, the numbers of analyzed ears were $n = 8$ for control, $n = 8$ for 2 h, $n = 8$ for 6 h, $n = 8$ for 12 h, $n = 8$ for 24 h, and $n = 9$ for 72 h after noise exposure. A mixture of nuclear extracts remaining after the EMSA analysis at each time point was used for supershift analysis of control, 2 h, and 12 h after noise exposure. For immunohistochemistry, the numbers of analyzed ears were $n = 2$ for control, $n = 2$ for 2 h, and $n = 2$ for 72 h after noise exposure.

4.2. *Noise exposure*

Mice were exposed to 124 dB SPL octave band noise, centered at 4 kHz, for 2 h, within a sound chamber. Each animal was placed in a cage. The sound chamber was fitted with a speaker driven by a noise generator (AA-67N; RION, Tokyo, Japan) and two power amplifiers (SRP-P150; SONY, Tokyo, Japan and D-1405; FOSTEX, San Angelo Drive Chesterfield, MO, USA). To ensure uniformity of the stimulus, sound levels were calibrated and measured using a sound level meter (NL-20; RION, Tokyo, Japan). The sound level meter was positioned at the level of the animal's head.

4.3. *Auditory brainstem response recording*

For ABR measurement, stainless steel needle electrodes were placed at the vertex and ventro-lateral to the left and right ears. Electroencephalogram recording was performed using the extracellular amplifier Digital Bioamp system (BAL-1; Tucker-Davis Technologies, FL, USA), and waveform storing and stimulus control were performed using Scope software of PowerLab system (PowerLab 2/20; ADInstruments, Castle Hill, Australia). Sound stimuli were produced by a coupler type speaker (ES1spc;

BioResearchCenter, Nagoya, Japan) inserted into the external auditory canal of a mouse. Tone burst stimuli, 0.1 ms rise/fall time (cosine gate) and 1 ms flat segment, were generated using Real-Time Processor (RP2.1; Tucker-Davis Technologies, FL, USA), and the amplitudes were specified by a Programmable Attenuator (PA5; Tucker-Davis Technologies, FL, USA). Sound levels were calibrated using a sound level meter (LA-5111; Ono Sokki, Yokohama, Japan). ABR waveforms were recorded for 12.8 ms at a sampling rate of 40,000 Hz using 50–5000 Hz bandpass filter settings. Waveforms from 1024 stimuli at a frequency of 9 Hz were averaged. For recording, animals were anesthetized (80 mg/kg ketamine, 15 mg/kg xylazine, i.p.). The thresholds of ABR were determined before noise exposure and 2 h, 6 h, 12 h, 24 h, or 72 h afterward at 4, 12, and 20 kHz, using a 5-dB SPL minimum step size down from a maximum amplitude. The hearing threshold was defined as the lowest stimulus intensity that produced a reliable wave III of ABR. Because the constraining test tones were set to SPLs of less than 89.7, 86.7, and 85 dB at 4, 12, and 20 kHz, respectively, the thresholds were recorded as 94.7, 91.7, and 90 dB respectively for the calculation of the threshold shift value when there was no response due to profound hearing impairment.

4.4. *Surface preparation*

Surface preparations were carried out to ensure whether this noise condition damaged the cochlea. The numbers of analyzed ears were $n = 1$ for control, $n = 2$ for 2 h, and $n = 2$ for 72 h after noise exposure. These animals were not used for other procedures. The auditory bullae were quickly removed, and the inner ear was transferred into 4% paraformaldehyde (PFA). The bones near the apex of the cochlea as well as the round window and oval window were opened followed by perilymphatic perfusion with 4% PFA. After overnight fixation at 4 °C, the inner ears were decalcified in 0.1 M EDTA for 7 days. After removal of the bony capsule and the lateral wall tissues, the OC was removed from the temporal bone. Tissue was incubated in 0.3% Triton X-100 in PBS for 7 min. The OC was incubated with flourescein phalloidin (F-432; Molecular Probes, Eugene, OR, USA; 1:50) overnight to outline hair cells. After three PBS rinses, the OC was incubated with propidium iodide (PI) (P-3566; Molecular Probes; 1:250) for 15 min to evaluate nuclear morphology. After three PBS rinses, it was mounted as a surface preparation. The areas around 25% and 50% of the distance from the apex, which are known to be the most stimulated regions by the 4 kHz and 10 kHz sounds, respectively (Ou et al., 2000), were observed. The area that was 70% of the distance from the apex, which is known to be vulnerable to noise exposure regardless of the center frequency of the octave band noise (Ou et al., 2000; Wang et al., 2002), was also observed. Immunolabeling was visualized using epi-fluorescence microscopy.

4.5. *Sample preparation for EMSA*

Mice were immediately decapitated under deep anesthesia after ABR measurements, and then the cochleas were dissected to prepare nuclear extracts according to Schreiber et al. (1989) with minor modifications (Ogita et al., 2000). In brief, tissues were homogenized in 10 mM sodium HEPES (pH 7.9) containing 10 mM KCl, 1 mM EDTA, 1 mM EGTA, 5 mM dithiothreitol, the phosphatase inhibitors (10 mM sodium β-glycerophosphate and 1 mM sodium orthovanadate), and 1 μg/ml each of the protease inhibitors (p-amidinophenyl) methanesulfonyl fluoride, benzamidine, leupeptin, and antipain. After the addition of Nonidet P-40 at a final concentration of 0.5%, the homogenates were centrifuged at 15,000 × g for 5 min to pellet a nuclei-containing fraction. The pellets were suspended in 50 mM Tris–HCl (pH 7.5) containing 10% glycerol, 400 mM NaCl, 1 mM EDTA, 1 mM EGTA, 5 mM dithiothreitol, and the phosphatase and protease inhibitors as above and kept on ice for 30 min. The suspensions were then centrifuged at 15,000 × g for 5 min, and the supernatant nuclear extracts were stored at −80 °C until assay.

4.6. *NF-κB/DNA binding mobility shift assays*

Oligonucleotides containing the NF-κB binding sequence from the murine κ-immunoglobulin light chain gene enhancer, 5′-AGTT-GAGGGGACTTTCCCAGG-3′, and its complementary sequence were annealed as a probe for the EMSA. The probe was labeled with [α-^{32}P]deoxy-ATP (PerkinElmer Life Sciences, Inc., MA, USA) using Klenow fragment of DNA polymerase I in 10 mM Tris–HCl buffer (pH 7.5) containing 50 mM NaCl, 10 mM $MgCl_2$, and 1 mM DTT at 25 °C for 30 min in the presence of 50 μM each of deoxy-GTP, deoxy-CTP, and deoxy-TTP. Aliquots (5 μg of protein) of nuclear extracts were incubated with 50 fmol probe (0.5–5 × 10^6 cpm/pmol) in 20 μL 50 mM Tris–HCl buffer (pH 7.5) containing 1 μg poly(dI–dC), 10% (vol/vol) glycerol, 10 mM $MgCl_2$, 160 mM NaCl, 1 mM EDTA, 1 mM EGTA, 5 mM DTT, 5 mM each of the aforementioned phosphatase inhibitors, and 1 μg/mL each of the protease inhibitors for 30 min at 2 °C. Bound and free probes were separated by electrophoresis on a 5% (wt/vol) polyacrylamide gel in buffer (pH 8.5) containing 50 mM Tris, 0.38 M glycine, and 2 mM EDTA at a constant voltage of 11 V/cm for 1.5 h in an ice bath. Gels were fixed, dried, and exposed to X-ray films for different periods to obtain autoradiograms most adequate for subsequent quantitative densitometry.

4.7. *Determination of NF-κB protein component by supershift analysis*

The composition of proteins bound to the DNA probe was analyzed by preincubation of nuclear extracts with antibodies against individual components of the NF-κB protein family including p50 and p65 proteins. Antibodies against p50 (sc-7178; Santa Cruz Biotechnology Inc., Santa Cruz, CA, USA; 3 μg) or p65 (sc-109-G; Santa Cruz Biotechnology Inc.; 3 μg) were added into the incubation mixture and allowed to react at 4 °C for 14–16 h. Samples were then subjected to electrophoresis (as described above), and autoradiograms were analyzed for supershift of the bound probe to a more slowly migrating position due to antibody association with the complex (Ogita et al., 1996).

4.8. *Data analysis and statistics*

Densitometric analysis for quantification of autoradiograms was carried out with the aid of Atto Densitograph (Atto Co., Tokyo, Japan). Values for each tissue were calculated as the percentage of NF-κB/DNA binding in noise-exposed mice compared with untreated mice and are expressed as the mean ± SE. Statistical significance was determined by Student's t test using Stat-View software (SAS Institute, Inc., Cary, NC, USA), and differences with P value less than 0.05 were considered significant.

4.9. *Immunohistochemistry for NF-κB*

For immunohistochemistry, mice were immediately decapitated under deep anesthesia after ABR measurements. The auditory bullae were quickly removed and the inner ear transferred into 4% PFA. Perilymphatic perfusion with 4% PFA was performed as described above. After overnight fixation at 4 °C, the inner ears were decalcified in 0.1 M EDTA for 7 days and embedded in paraffin using routine procedures and sectioned at 4 μm thickness. The slides were dewaxed in xylene, rehydrated through graded ethanol, and quenched with 3% H_2O_2 in methanol for 30 min. After antigen retrieval by heat treatment in 10 mM citrate buffer (pH 6.0) at 105 °C for 45 min, they were quenched with 0.1% avidin for 20 min, 0.01% biotin for 20 min, and 1% casein for 30 min.

Immunolabeling was carried out overnight at 4 °C with an anti-p65 antibody (sc-372; Santa Cruz Biotechnology Inc.; 1:50) or an anti-p50 antibody (KAP-TF112; Stress Gen Biotechnologies Corp., Glanford Avenue Victoria, BC, Canada; 1:200), and then the slides were incubated for 30 min in biotinylated anti-goat IgG antibody (AP106B; Chemicon International, Temecula, CA, USA; 1:200) for p65 and in biotinylated anti-rabbit IgG antibody (BA-1000; Vector Laboratories, Burlingame, CA, USA; 1:200) for p50 at room temperature. Finally, the slides were incubated for 30 min in Streptavidin ABComplex/HRP (K0377; Dako, Glostrup, Denmark; 1:100). Reaction products were developed using 3′,5′-diaminobenzidine as a substrate for peroxidase. Sections were nuclear stained with hematoxylin. All of the washes were performed in 0.1 mM Tris-buffered saline (0.3M NaCl, 0.1% Tween20, 0.1 M Tris–HCl buffer) (pH 7.6) except for the wash after incubation in Streptavidin ABComplex/HRP. Tris-buffered saline of 50 mM (pH 7.6) was used for this wash.

4.10. *Immunohistochemistry for p65 and iNOS*

The paraffin slides, which were made in the above procedure, were dewaxed. After antigen retrieval by heat treatment in 10 mM citrate buffer (pH 6.0) at 105 °C for 30 min, they were incubated in blocking solution consisting of 1% casein for 30 min.

Immunolabeling was carried out for 1 h in room temperature with an anti-p65 antibody, and then the slides were incubated for 1 h in Alexa Fluor 488-conjugated rabbit anti-goat IgG secondary antibody (A-11078; Molecular Probes; 1:200). Next, immunolabeling for iNOS was carried for 1 h with an anti-iNOS antibody (SA-200; BIOMOL International, Plymouth Meeting, PA, USA; 1:500), and then the slides were incubated for 1 h in Alexa Fluor 546-conjugated F(ab′) fragment of goat anti-rabbit IgG secondary antibody (A-11071; Molecular Probes; 1:200). Sections were nuclear stained with hematoxylin. All of the washes were performed in 0.1 mM Tris-buffered saline (pH 7.6). Immunolabeling was visualized using confocal microscopy.

4.11. *Animal use and care*

All experimental protocols were in compliance with guidelines of the National Institutes of Health and the Declaration of Helsinki, and all procedures were approved and supervised by the Keio University Union on Laboratory Animal Medicine.

Acknowledgment

The author would like to thank Mr. Takashi Kimura for his assistance in immunohistochemistry.

REFERENCES

Bohne, B.A., Rabbitt, K.D., 1983. Hear. Res. 11, 41–53.
Bowie, A., O'Neill, L.A., 2000. Biochem. Pharmacol. 59, 13–23.
D'Acquisto, F., May, M.J., Ghosh, S., 2002. Mol. Interv. 2, 22–35.
Denk, A., Wirth, T., Baumann, B., 2000. Cytokine Growth Factor Rev. 11, 303–320.
Fujioka, S., Niu, J., Schmidt, C., Sclabas, G.M., Peng, B., Uwagawa, T., Li, Z., Evans, D.B., Abbruzzese, J.L., Chiao, P.J., 2004. Mol. Cell. Biol. 24, 7806–7819.
Garside, H., Stevens, A., Farrow, S., Normand, C., Houle, B., Berry, A., Maschera, B., Ray, D., 2004. J. Biol. Chem. 279, 50050–50059.
Ghosh, S., May, M.J., Kopp, E.B., 1998. Annu. Rev. Immunol. 16, 225–260.
Handel, M.L., 1997. Inflamm. Res. 46, 282–286.
Hirose, K., Liberman, M., 2003. J. Assoc. Res. Otolaryngol. 4, 339–352.
Hsu, C.J., Shau, W.Y., Chen, Y.S., Liu, T.C., Lin-Shiau, S.Y., 2000. Hear. Res. 142, 203–211.
Hsu, W.C., Wang, J.D., Hsu, C.J., Lee, S.Y., Yeh, T.H., 2004. Acta Oto-Laryngol. 124, 459–463.
Hu, B.H., Henderson, D., Nicotera, T.M., 2002. Hear. Res. 166, 62–71.
Ichimiya, I., Yoshida, K., Hirano, T., Suzuki, M., Mogi, G., 2000. Int. J. Pediatr. Otorhinolaryngol. 56, 45–51.
Jacono, A.A., Hu, B., Kopke, R.D., Henderson, D., Van De Water, T.R., Steinman, H.M., 1998. Hear. Res. 117, 31–38.
Jager, W., Goiny, M., Herrera-Marschitz, M., Brundin, L., Fransson, A., Canlon, B., 2000. Exp. Brain Res. 134, 426–434.
Jiang, H., Sha, S.H., Schacht, J., 2005. J. Neurosci. Res. 79, 644–651.
Keynes, R.G., Garthwaite, J., 2004. Curr. Mol. Med. 4, 179–191.
Kikuchi, T., Kimura, R.S., Paul, D.L., Takasaka, T., Adams, J.C., 2000. Brain Res. Brain Res. Rev. 32, 163–166.
Li, H.S., Niedzielski, A.S., Beisel, K.W., Hiel, H., Wenthold, R.J., Morley, B.J., 1994. Hear. Res. 78, 235–242.
Matsunobu, T., Ogita, K., Schacht, J., 2004. Neuroscience 123, 1037–1043.
Mattson, M.P., Culmsee, C., Yu, Z., Camandola, S., 2000a. J. Neurochem. 74, 443–456.
Mattson, M.P., Culmsee, C., Yu, Z.F., 2000b. Cell Tissue Res. 301, 173–187.
Merchant, S.N., Adams, J.C., Nadol Jr., J.B., 2005. Otol. Neurotol. 26, 151–160.
Minami, S.B., Yamashita, D., Schacht, J., Miller, J.M., 2004. J. Neurosci. Res. 78, 383–392.
Mori, T., Fujimura, K., Yoshida, M., Suzuki, H., 2004. Auris, Nasus, Larynx 31, 395–399.
Nakashima, T., Naganawa, S., Sone, M., Tominaga, M., Hayashi, H., Yamamoto, H., Liu, X., Nuttall, A.L., 2003. Brain Res. Brain Res. Rev. 43, 17–28.
Ogita, K., Amizuka, T., Azuma, Y., Yoneda, Y., 1996. Neurochem. Res. 21, 201–209.
Ogita, K., Matsunobu, T., Schacht, J., 2000. NeuroReport 11, 859–862.
Ohinata, Y., Miller, J.M., Altschuler, R.A., Schacht, J., 2000. Brain Res. 878, 163–173.
Ohinata, Y., Miller, J.M., Schacht, J., 2003. Brain Res. 966, 265–273.
Ohlemiller, K.K., Wright, J.S., Dugan, L.L., 1999. Audiol. Neuro-Otol. 4, 229–236.
Ou, H.C., Harding, G.W., Bohne, B.A., 2000. Hear. Res. 145, 123–129.
Pryor, W.A., Lemercier, J.N., Zhang, H., Uppu, R.M., Squadrito, G.L., 1997. Free Radical Biol. Med. 23, 331–338.
Rahman, I., Marwick, J., Kirkham, P., 2004. Biochem. Pharmacol. 68, 1255–1267.
Ramkumar, V., Whitworth, C.A., Pingle, S.C., Hughes, L.F., Rybak, L. P., 2004. Hear. Res. 188, 47–56.
Schreiber, E., Matthias, P., Muller, M.M., Schaffner, W., 1989. Nucleic Acids Res. 17, 6419.
Sha, W.C., 1998. J. Exp. Med. 187, 143–146.
Shi, X., Nuttall, A.L., 2003. Brain Res. 967, 1–10.
Shi, X., Ren, T., Nuttall, A.L., 2002. Hear. Res. 164, 49–58.
Shi, X., Dai, C., Nuttall, A.L., 2003. Hear. Res. 177, 43–52.
Shizuki, K., Ogawa, K., Matsunobu, T., Kanzaki, J., Ogita, K., 2002. Neurosci. Lett. 320, 73–76.
Spicer, S.S., Schulte, B.A., 1996. Hear. Res. 100, 80–100.
Suko, T., Ichimiya, I., Yoshida, K., Suzuki, M., Mogi, G., 2000. Hear. Res. 140, 137–144.
Takemura, K., Komeda, M., Yagi, M., Himeno, C., Izumikawa, M., Doi, T., Kuriyama, H., Miller, J.M., Yamashita, T., 2004. Hear. Res. 196, 58–68.
Takumida, M., Anniko, M., 2001. Acta Oto-Laryngol. 121, 342–345.
Wang, Y., Liberman, M.C., 2002. Hear. Res. 165, 96–102.
Wang, Y., Hirose, K., Liberman, M.C., 2002. J. Assoc. Res. Otolaryngol. 3, 248–268.

Watanabe, K., Inai, S., Jinnouchi, K., Bada, S., Hess, A., Michel, O., Yagi, T., 2002. Anticancer Res. 22, 4081–4085.
Wooten, M.W., 1999. J. Neurosci. Res. 58, 607–611.
Xu, J., Fan, G., Chen, S., Wu, Y., Xu, X.M., Hsu, C.Y., 1998. Brain Res. Mol. Brain Res. 59, 135–142.
Yamane, H., Nakai, Y., Takayama, M., Konishi, K., Iguchi, H., Nakagawa, T., Shibata, S., Kato, A., Sunami, K., Kawakatsu, C., 1995. Acta Oto-Laryngol., Suppl. 519, 87–92.
Yamasoba, T., Harris, C., Shoji, F., Lee, R.J., Nuttall, A.L., Miller, J.M., 1998. Brain Res. 804, 72–78.

WILEY InterScience® DISCOVER SOMETHING GREAT

Journal of Neuroscience Research 83:575–583 (2006)

Proinflammatory Cytokines Expression in Noise-Induced Damaged Cochlea

Masato Fujioka,[1,2] Sho Kanzaki,[1] Hirotaka James Okano,[2,3] Masatsugu Masuda,[1] Kaoru Ogawa,[1] and Hideyuki Okano[2,3]*

[1]Department of Otolaryngology, Head and Neck Surgery, Keio University School of Medicine, Tokyo, Japan
[2]Department of Physiology, Keio University School of Medicine, Tokyo, Japan
[3]Solution Oriented Research for Science and Technology (SORST), Saitama, Japan

Recent studies have showed that inflammatory responses occur in inner ear under various damaging conditions including noise-overstimulation. We evaluated the time-dependent expression of proinflammatory cytokines in noise-exposed rat cochlea. Among several detected cytokines, real-time RT-PCR showed that interleukin-1beta (IL-1β) and interleukin-6 (IL-6) were significantly induced 3 hr after noise exposure, and quickly downregulated to the basal level. Tumor necrosis factor-alpha (TNF-α) was also slightly upregulated immediately after noise exposure. Immunohistochemical analysis showed that IL-6 expression was distinctively induced within the lateral side of the spiral ligament. Sequential expression analysis showed that IL-6 immunoreactivity was initially found in the cytoplasm of lateral wall cells, including Type IV and III fibrocytes, and expanded broader throughout the lateral wall, finally to the stria vascularis. Because of the negative Iba-1 staining, IL-6 expression in the early-phase was not due to macrophage or microglia activation. IL-6 was also detected in spiral ganglion neurons at 12 and 24 hr after noise exposure. Our data demonstrates the production of proinflammatory cytokines, including TNF-α, IL-1β, and IL-6, in early phase of noise overstimulated cochlea. IL-6 expression was observed in the spiral ligament, stria vascularis, and spiral ganglion neurons. These cytokines, produced by the cochlear structure itself in response to noise exposure, may initiate an inflammatory response and have some role in the mechanism of noise-induced cochlear damage.

Key words: cochlea damage; inflammation; cytokines; gene expression; hearing

Overexposure to high intense noise is a well known cause of sensorineural hearing loss, clinically and experimentally. Researchers have focused their attention on the pathology of hair cells in noise-induced hearing loss (NIHL) due to the overstimulation of hair cells. However, several recent studies showed the histopathology of nonsensory cells, including lateral wall fibrocytes and stria cells (Hirose and Liberman, 2003), which suggests that alternative pathophysiology and/or physiological responses to noise over-stimulation may also be involved in NIHL. Interestingly, not only their morphological changes including degenerative processes were seen in these cochlea non-sensory cells: the infiltration of monocytes was also observed by histological evaluation (Hirose et al., 2005), suggesting that an early-phase inflammatory response may be involved in noise over-stimulated damage in cochleae.

Fibroblast is generally known as a key regulator in inflammation, inducing secondary inflammatory responses by producing several cytokines, and closing local inflammation with remodeling; as its disorders lead to excessive inflammation (Buckley et al., 2001; Mor et al., 2005). Cochlear lateral wall fibrocytes are also known to produce inflammatory mediators, as shown by several studies. For example, several in vitro studies have reported that cultured cochlear lateral wall fibrocytes produced IL-6 and other inflammatory agents, including chemoattractants for inflammatory cells, when stimulated by IL-1β or TNF-α (Yoshida et al., 1999; Ichimiya et al., 2000). Concomitantly, experimental inner ear inflammation studies have shown the in vivo production of TNF-α, IL-1β, and IL-6 in cochleae, along with synergic leukocyte infiltration; both of these processes were enhanced by lipopolysaccharide (LPS) intraperitoneal injections (Satoh et al., 2003; Hashimoto et al., 2005). In addition, an in vivo loss of function analysis demonstrated that TNF-α was a deteriorating factor for cochlea inflammation (Satoh et al., 2002). These studies are very important because such molecules are, in general, well known for their potential to induce secondary inflammatory responses, including leukocyte infiltration, scar formation, or gliosis in other injured

Contract grant sponsor: Keio University Grant-in-Aid for Encouragement of Young Medical Scientists; Contract grant sponsor: Japanese Ministry of Education, Culture, Sports, Science and Technology.

*Correspondence to: Hideyuki Okano, Department of Physiology Keio University School of Medicine, 35 Shinanomachi, Shinjuku-ku, Tokyo, 160-8582, Japan. E-mail: hidokano@sc.itc.keio.ac.jp

Received 2 December 2005; Revised 30 November 2005; Accepted 30 November 2005

Published online 20 January 2006 in Wiley InterScience (www.interscience.wiley.com). DOI: 10.1002/jnr.20764

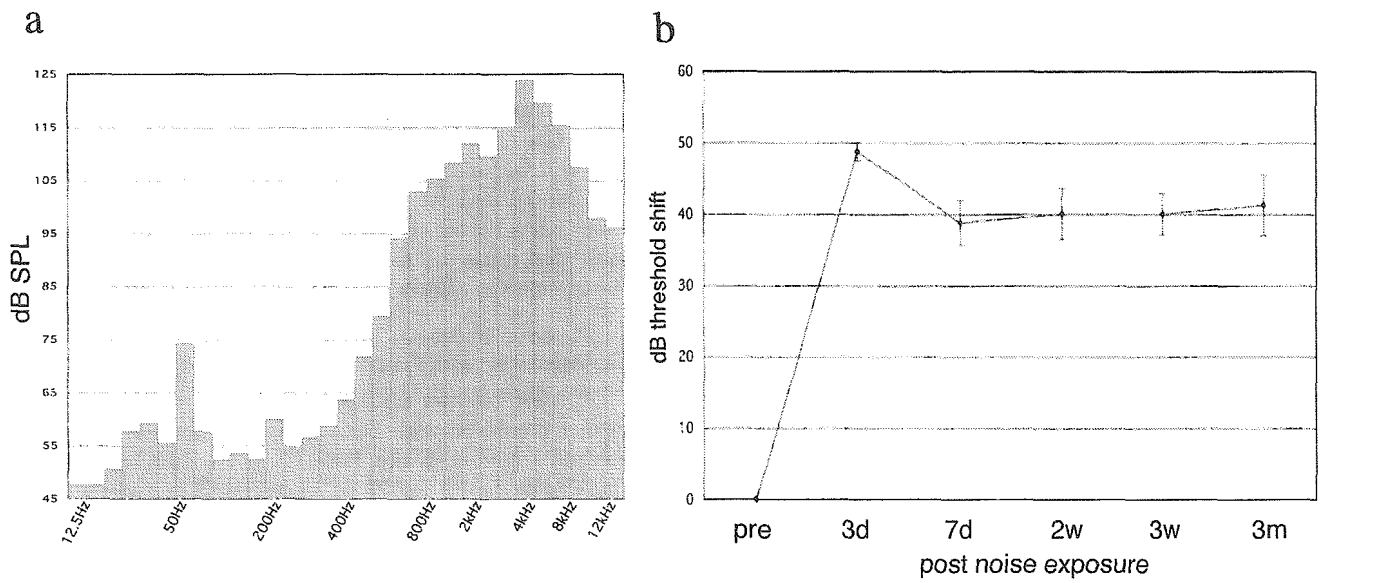

Fig. 1. Noise-induced hearing loss (NIHL) model. Overexposure to large amounts of sound causes hearing loss, but the hearing impairment level depends on the sound intensity, the types of sound, and the susceptibility of the animals. **a:** Sound spectrum used in the experiment, a one-octave-band noise centered at 4 kHz, 124 dB SPL. **b:** Threshold shift we obtained in this experiment ($n = 4$). The hearing level was measured by determining the auditory brain-evoked response (ABR) threshold, and the threshold shift from the pre-noise exposure was defined as the impaired level of hearing. The resulting shift persisted for up to 3 months, with a final shift of 41.3 ± 4.27 dB (mean ± SEM).

organs. These reports indicate the involvement of proinflammatory cytokines in cochlear damage. If the expression of proinflammatory cytokines is demonstrated in cochlea in other models, some physiological or pathophysiological meanings may exist. Evidence of proinflammatory cytokines expression in cochlea has restricted to experimental inflammation or autoimmune diseases. In noise-induced damaged cochlea, the expression of proinflammatory cytokines has not yet been clarified, even though the existence of active inflammatory cells has been reported (Hirose et al., 2005). Considering this background, determining the expression of proinflammatory cytokines under noise-stimulated conditions may help us to understand the early phase of inflammation in NIHL, both physiologically and pathophysiologically. In the present study, we evaluated the expression of cytokines in cochlea using RT-PCR. In addition, we carried out an immunohistochemistry analysis to determine the distribution of IL-6 expression in cochleae after noise exposure.

MATERIALS AND METHODS

Animal Preparation

Four-to-six-week-old male Sprague-Dawley (SD) rats with normal Preyer reflexes were used ($n = 50$). The animals were purchased from Saitama-Experimental Animal Center and were bred in Laboratory Animal Center, School of Medicine, Keio University under SPF conditions. All procedures were approved by the ethics committee of Keio University Union on Laboratory Animal Medicine in accordance with the Guide for the Care and Use of Laboratory Animals (National Institute of Health, Bethesda, MD).

Noise Exposure

In all the experiments, the animals were exposed for 2 hr to octave-band noise (OBN) with a peak at 4 kHz, 124 dBSPL. The noise was generated by an audiometer (AA-67N, RION, Tokyo, Japan) with a masking noise at 4 kHz and was amplified sequentially using two amplifiers: SRP-P150 (SONY, Tokyo, Japan) and D-1405 (FOSTEX, Chesterfield, MO). The animals and speakers were placed in the same box that had been used previously in our laboratory (Shizuki et al., 2002). To deliver the noise stimulation symmetrically in both ears, the animals were placed in the 12-cm diameter, barreled shape cage that was made with metallic mesh, right under the round-shaped speaker. Before the experiments, threshold shift of both ears in each animal were evaluated. No significant difference was observed between left and right ears ($n = 3$, data not shown). The noise conditions at the animals' location were evaluated before the experiments (Fig. 1a).

Auditory Brainstem-Evoked Response

To determine the magnification of the noise-induced hearing loss under the noise conditions in this study, we tested the threshold shift using the click-evoked auditory brainstem-evoked response (ABR). The ABR of the animals ($n = 4$) was determined 3 days before the noise exposure and 3 days, 1, 2, 3, and 4 weeks and 3 months after noise exposure. The ABR measurements were carried out using methods and equipment reported previously (Hoya et al., 2004). Instead of tone-burst stimuli, click stimuli were used in the present